NERC Scientific Support and Facilities
Ion Microprobe Facility

University of Edinburgh
NERC Ion Microprobe Facility
2024 Annual Science Report

Ion Microprobe Facility
School of Geosciences
Grant Institute
Kings Buildings
James Hutton Road
Edinburgh
EH9 3FE

https://www.ed.ac.uk/geosciences/about/facilities/all/ionprobe

Contents

Pinpointing the source of shallow slab fluid/volatiles release via B isotopes in melt inclusions from high MgO basalts across the Kamchatka Arc

E. Brennan[1], I. Savov[1], S. Agostini[2] , T. Churikova[3], A. Iveson[4] & J.C.M. De Hoog[5]

[1]School of Earth and Environment, University of Leeds, LS2 9JT, UK
[2]IGG Labs-CNR- Pisa, Italy
[3]Institute of Volcanology and Seismology FED RAS, Petropavlovsk-Kamchatsky, Russia
[4] Pacific Northwest National Laboratory, USA
[5] School of GeoSciences, University of Edinburgh, UK

Background

The subduction of the Mesozoic Pacific plate beneath Kamchatka provides an ideal setting to investigate volatile release across volcanic arcs. Boron's fluid mobility and extreme depletion in the subarc mantle make it an outstanding tracer for dehydration reactions taking place on the slab [1]. The global across arc pattern appears to show $\delta^{11}B$ ratios are becoming lighter and concentrations decrease as the subducted slabs dehydrate at depth. By analysing olivine-hosted melt inclusions (MI) from selected high-MgO basalts at the front arc Kozelsky and Avachinsky volcanoes, we assess the non-sediment-derived slab outfluxes at shallow mantle depths (~100km depth to slab) [2]. Additionally, this study contributes to the broader across-arc dataset [3, 4] by incorporating $\delta^{11}B$ measurements from several additional volcanoes (Figure 1), providing a more comprehensive understanding of the fate of volatiles across Kamchatka as an example of cold subduction zone [2].

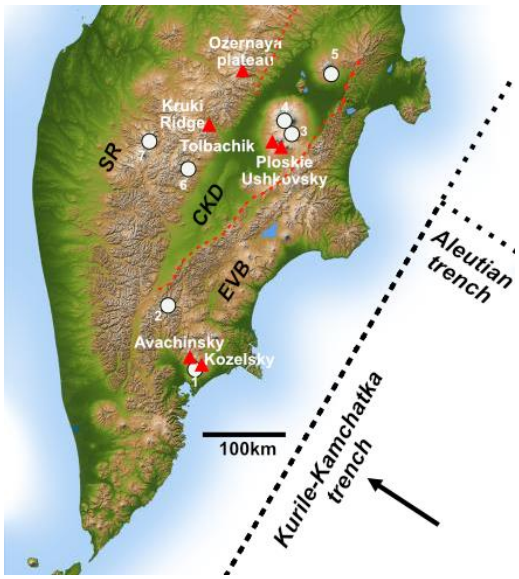

Fig. 1. Simplified location map of the Kamchatka Peninsula showing sample locations from this study (red triangles) and Iveson et al. [3] locations (white circles). Iveson et al. locations 1 to 7 are as follows: 1) Medvezhka, 2) Bakening, 3) Kamen, 4) Klyuchevskoy, 5) Shiveluch, 6) Achtang, 7) Ichinsky.

Samples were selected from 12 localities from seven volcanoes (Figure 1). Two localities from the Eastern Volcanic Belt (EVB), three from the Central Kamchatka Depression (CKD), and the remaining samples originate from the rear arc Sredinny Ridge (SR). These samples capture varying degrees of slab-fluid/melt release at different depths (90–350 km) [2]. MI were hosted in olivine from Mg-rich lavas and tephra. Whole-rock compositions from the same samples range from andesite to basalt, but the most mafic compositions were selected to eliminate any impact of AFC processes. A total of 59 large MI were analysed out of 68 MI in two grain mounts, with 42 successful measurements (see Fig. 2).

Results & Discussion

The $\delta^{11}B$ ratios in MI are expected to decrease with increasing slab depth, consistent with progressive slab dehydration [1, 4]. Despite some scatter, the dataset (Fig. 2) aligns closely with the whole-rock (WR) and MI data from Iveson et al. (2021) which includes an eight-volcano transect [3, 4]. The results indicate contributions from both dehydrated altered oceanic crust,~+3.4‰ (0 to +18), and oceanic serpentinite ~+12‰ (+7 to+20) sources supporting their key role for transporting boron and generating increasingly light boron to deep (lower) mantle [1,3,5].

The MI $\delta^{11}B$ ratios show far greater variability than the WR. Interestingly, the WR $\delta^{11}B$ ratios often average those of the MI. Kozelsky volcano- the primary focus of this study- displays a $\delta^{11}B$ range nearly as large as that observed across the entire Kamchatka arc. These findings support the conclusion by

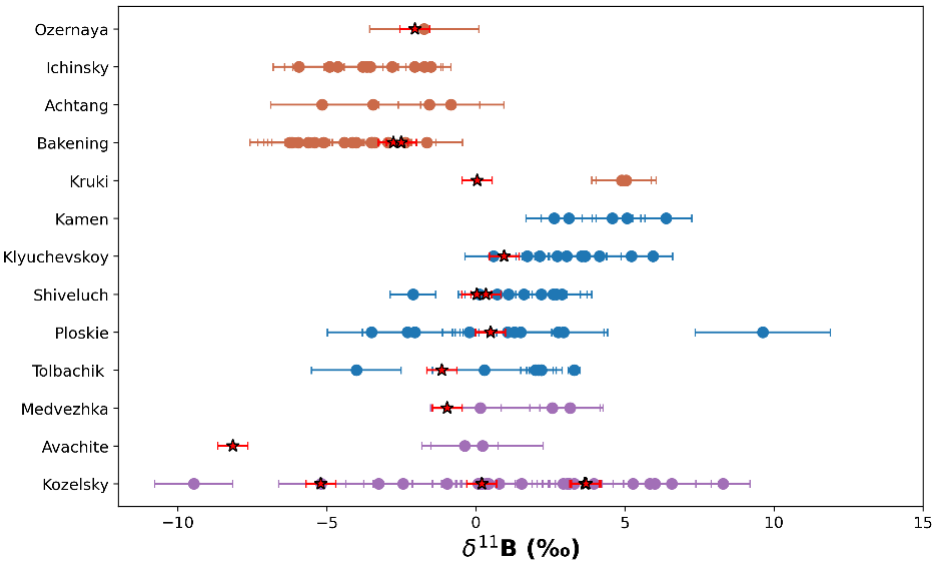

Fig. 2. MI (circles) and WR(stars) analyses. WR measurements following the method described in [7]. Colours corresponding to the volcanic regions: SR (orange), CKD (blue), and EVB (purple). Error bars represent 1σ uncertainty. Note: Avachite is an unusual sample from Avachinsky not reflective of the lavas or scoria.

Iveson et al. (2021) that MI preserve greater intra-sample δ^{11}B variability in comparison with the WR data from the same volcano [3]. This suggests that individual MIs capture snapshots of distinct stages or pathways of fluid/melt transport. The wide range in MI data—particularly the extremes—likely reflects melting and slab fluid components that are cryptic in the erupted WR products, preserving signals that were somehow filtered out or had never erupted.

Notably, no systematic correlation was observed between δ^{11}B and AFC processes at Kozelsky, indicating that crustal assimilation is not the primary control on boron systematics in this setting. This is also confirmed by the unradiogenic Sr and Nd isotopes of the WR. This further highlights the sensitivity of MI to early-stage devolatilization sources, which are often obscured in the WR records. The lack of correlation with AFC also supports the interpretation that boron isotope variations primarily reflect slab-derived signatures, strengthening the case for δ^{11}B as useful tracer of specific slab dehydration taking place at depth.

Several MI from back-arc settings yielded boron concentrations below detection limits (<10ppm, Cameca IMS 7f-Geo) preventing reliable δ^{11}B measurements. This observation is consistent with progressive boron depletion from the slab at greater depths. Meanwhile the EVB boron concentrations (~20-50ppm) are supporting a heavy and boron rich source in the forearc. Overall, samples from the SR exhibit isotopically lighter δ^{11}B values and low B contents (~<10ppm), consistent with and the proposed progressive depletion of boron at greater subduction depths [4, 6] especially when the anomalously high magmatic productivity and elevated δ^{11}B of the CKD are excluded. These results will be combined with WR B-Sr-Nd isotope systematics and trace element concentrations to further decipher the source of dehydrating lithologies of the slab i.e. hydrated basalts, hydrated gabbros, serpentinites on the slab and forearc and modified melange or mantle wedge rocks.

References

[1] J.C.M. De Hoog & I.P. Savov (2018) In: Marschall & Foster (Eds.), Boron Isotopes, Advances in Isotope Geochemistry, Springer, **217–247.** [2] T.G. Churikova et al. (2001) Journal of Petrology **42**, 1567–1593. [3] A.A. Iveson et al. (2021) Earth and Planetary Science Letters **562.** [4] T. Ishikawa et al. (2001) Geochimica et Cosmochimica Acta **65**, 4523–4537. [5] H.R. Marschall et al. (2017) Geochimica et Cosmochimica Acta **207**, 102–138. [6] M. Konrad-Schmolke et al. (2016) Geochemistry, Geophysics, Geosystems **17**. [7] S. Agostini et al. (2021) *Scientific Reports* **11**, 11230.

Constraining the primary sulphur concentration and isotopic composition of the Troodos ophiolite by analysis of volcanic glasses

G. Bromiley[1], L. Saper[1,2]

[1]School of GeoSciences, University of Edinburgh, Edinburgh EH9 3JW, UK
[2]Present Address: Jet Propulsion Laboratory, California Institute of Technology, Pasadena, CA, USA

Sulphur isotope data were collected on 35 Troodos Ophiolite glasses by over 5 days in April 2024 using the Cameca IMS-1270. The glasses had been previously measured for H_2O contents by in June 2023 using the 7f-GEO. **Figure 1** shows that the SIMS determined S and H_2O concentrations are in very good agreement with previous determinations by electron microprobe (S) and FTIR (H_2O) [1].

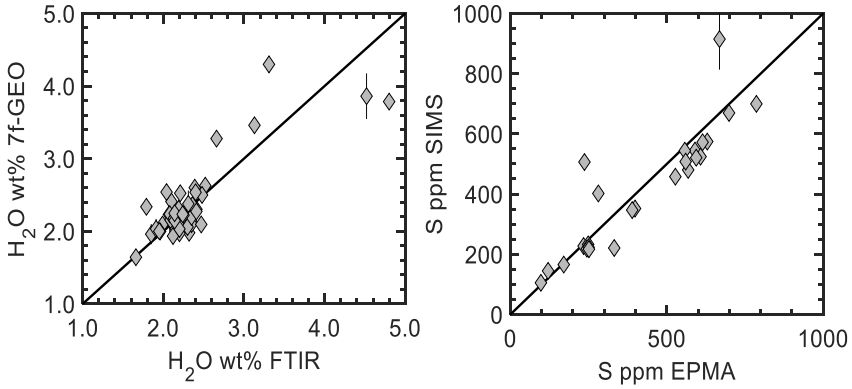

Fig. 1. H_2O and S determined in the same glasses by multiple techniques. Left: FTIR vs. SIMS. Right: EPMA vs. SIMS.

We used internal S-isotope glass standards A-35 and STAP [2] to correct for signal drift with time and for instrumental mass fractionation. **Figure 2** shows glass S versus $\delta^{34}S$ (per mil, relative to V-CDT), color-coded by sampling location. Glass $\delta^{34}S$ values range from –2.8±0.7‰ to +1.4±0.3‰. The majority of the glasses (24 of 35) have $\delta^{34}S$ values between –1‰ and +1‰, and all but two glasses overlap with this range within error. Excluding the four glasses from Limni and Arakapas with $\delta^{34}S < -2$‰, the average and standard deviation of average $\delta^{34}S$ values is +0.13 ±0.75‰, 1σ. This represents a direct measurement of the primordial S isotope composition of the Troodos Ophiolite and is in agreement with previous inferences based on whole rock measurements of altered cumulate rocks [3]). Such information is critical for modelling of S cycling in the Troodos Ophiolite, with implications for metal cycling and the formation of massive sulphide deposits.

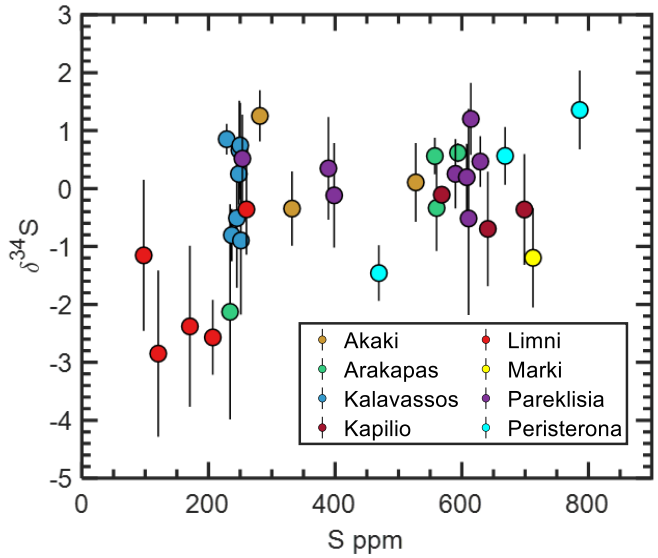

Fig. 2. Sulphur ppm versus $\delta^{34}S$ measured in glasses.

This S isotope value overlaps with MORB and is relatively light compared to previous determinations of S isotopes in Troodos Ophiolite rocks and sulphides by bulk extraction techniques (**Figure 3**). It is also light relative to values measured in glasses

in subduction zones. The heavy $\delta^{34}S$ measured in arc glasses has been interpreted to represent recycling of oxidized sulphate from the slab into the mantle wedge. The Troodos Ophiolite provides geochemical evidence for a significant subduction influence. However, our recent study shows that the volcanic glasses from Troodos are reduced relative to arcs, and overlap with MORB [4].

Our new S isotope data corroborate this interpretation, i.e., that the redox state in the Troodos Ophiolite is decoupled from its subduction influence due to very dilute S concentrations in the metasomatic agent. The origin of S in the Troodos Ophiolite and its variability is mostly inherited from the residual and depleted mantle left behind from previous melting events. We find petrographic evidence that this mantle was variable sulphide-saturated and that fractional melts mixed prior eruption. Troodos magmas were endowed with high-H_2O and fluid-mobile elements by fluxing of fluids that contained very low concentrations of sulphur, indicating that they likely formed close to the paleo-Tethyan trench.

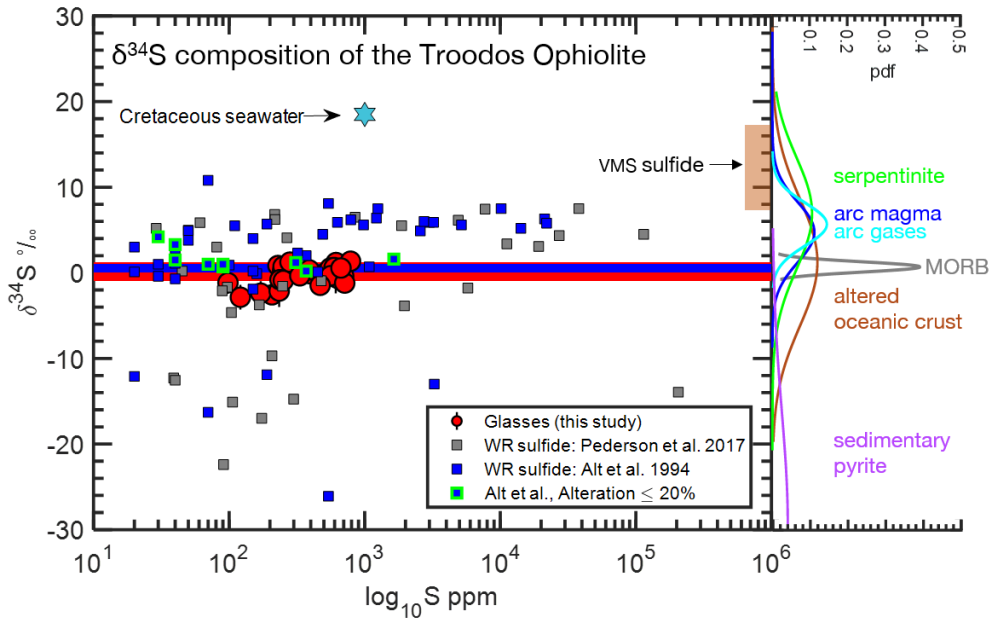

Fig. 3. Sulphur ppm (log-scale) vs. $\delta^{34}S$ of whole rocks, sulphides and glasses from the Troodos Ophiolite. Our data are the red circles and the red bar indicates 2 standard deviations about the mean. Also included are pdf functions of the distributions of $\delta^{34}S$ from various geological settings, as compiled in [5].

References

[1] D. Woelki et al. (2020) Lithos **356–357**, 105299.
[2] Taracsák et al. (2021) Chemical Geology **578**, 120318.
[3] Alt (1994) Geochimica et Cosmochimica Acta **58**, 1825–1840.
[4] Saper et al. (2024) Earth and Planetary Science Letters **627**, 118560.
[5] Muth and Wallace (2021) Geology **49**, 1177–1181.

Pre-eruptive volatile conditions in a crystal mush as recorded by apatite

G. Brown[1], M.C.S Humphreys[1], D.J Colby[1], V.C Smith[2] & J.C.M De Hoog[3]

[1]Department of Earth Sciences, Durham University, Durham DH1 3LE
[2]School of Archaeology, University of Oxford, Oxford, OX1 3TG
[3]School of GeoSciences, University of Edinburgh, Edinburgh EH9 3FE, UK

Introduction

Magmas are thought to be stored in the Earth's crust as crystal mushes, bodies consisting of a solid crystalline framework containing melt in its pore spaces. It is currently not well understood which processes contribute to the remobilisation and eruption of crystal mushes. Further investigation of this process might reveal triggers of highly explosive volcanic eruptions and facilitate more accurate eruption forecasting. This project aims to explore the role of magmatic volatiles in mush remobilisation, namely the timing of the onset of volatile saturation within the mush system. This is achieved by use of the apatite volatile record. Apatite incorporates key magmatic volatile species (H_2O, F, Cl) into its crystal structure; these species form a ternary exchange system, maintaining equilibrium with the volatile state of the melt until the apatite crystal is isolated from it [1], for example as a mineral inclusion. As the system evolves, apatite records the changing magmatic volatile conditions and can be used to interpret them, as well as identify the onset of volatile exsolution [1,2]. This study considers the volatile record of apatite inclusions present across a range of phenocrysts from the pyroclastic deposits of Las Cañadas Caldera (LCC), Tenerife.

Results and discussion

The Cameca 7f IMS-geo ion microprobe was used to obtain volatile data from apatite inclusions. Direct measurements of OH reveal vacancies on the apatite channel volatile site, leading to overestimation of water contents when determining OH through stoichiometry alone (Fig. 1). This highlights the need for direct measurement of volatile species in apatite. Volatile data were used in conjunction with selected trace elements (EPMA) and major element chemistry of the host minerals (SEM-EDS) to investigate the relationship between volatile state and degree of fractionation. In agreement with previous petrological studies of the LCC eruptions [3,4] three distinct magma compositions were present in the magmatic system at the time of eruption: phonolite 1, phonolite 2, and phonotephrite. Host mineral chemistry was used to determine which magma component the apatite inclusions were derived from, and apatite MgO contents were used to identify the fractionation trend within each component. The data show that each magma component was stored in a different volatile state prior to eruption. The phonotephrite shows increasing values of X_F/X_{OH} and X_{Cl}/X_{OH} with decreasing MgO contents, interpreted as increasing magma fractionation (Fig. 2; bottom). Increases in

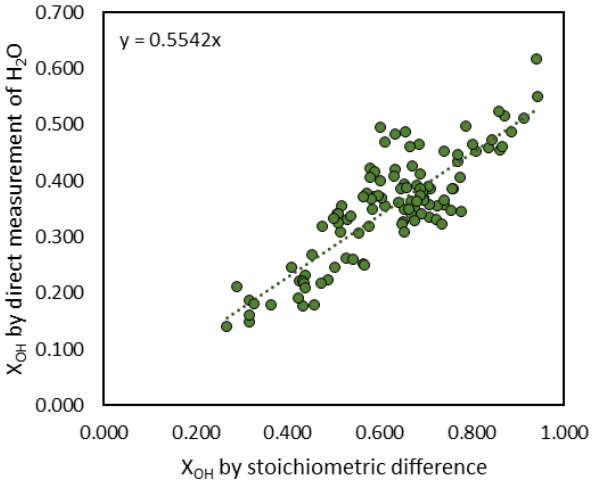

Fig. 1. comparison of OH determined by calculating the difference between the total capacity of the apatite volatile site (EPMA) and by direct measurement of OH by SIMS. Values "by difference" are overestimated compared to direct measurements.

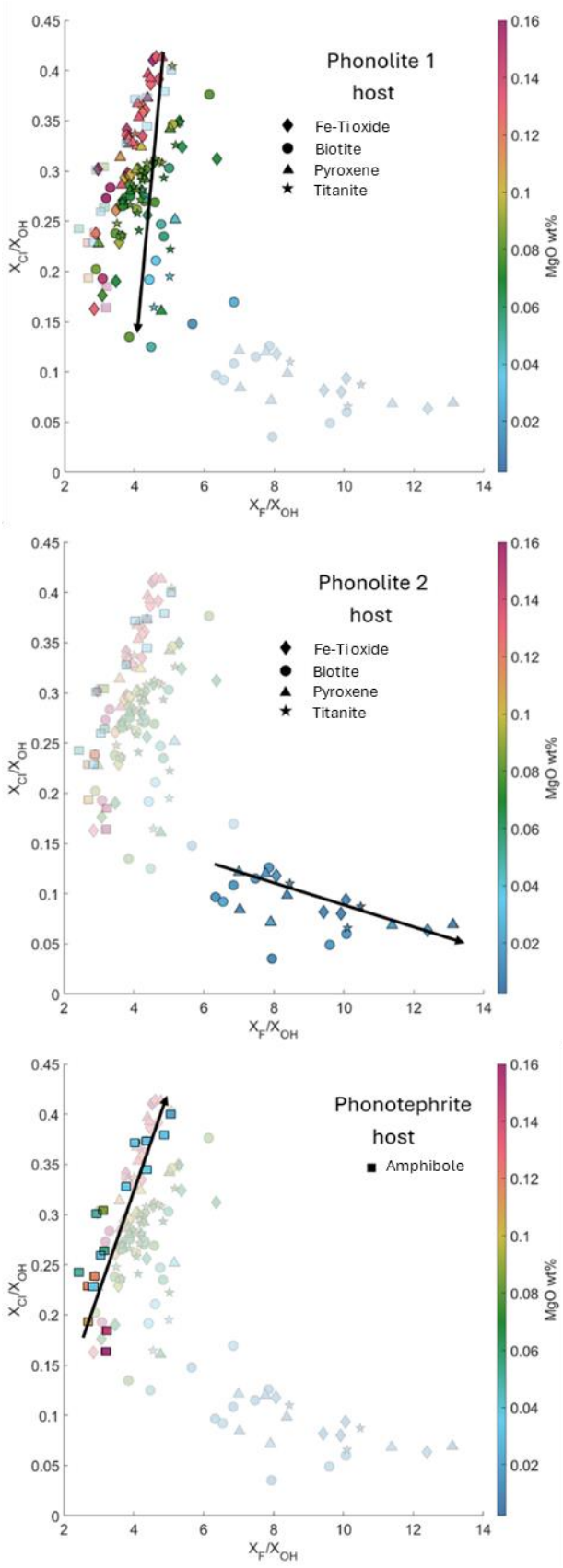

these ratios are interpreted as volatile enrichment in the melt due to fractionation. Chlorine preferentially partitions into an aqueous volatile phase if it is present, leading to a decrease in melt Cl contents, so the progressive increase in X_{Cl}/X_{OH} is considered to show that volatile saturation had not yet been achieved in the phonotephrite. The phonolite 1 magma shows a trend of decreasing X_{Cl}/X_{OH} with decreasing MgO (Fig. 2; top), interpreted as volatile exsolution during fractionation in a volatile-saturated magma. The phonolite 2 magma has much lower X_{Cl}/X_{OH} compared to phonolite 1 and shows increasing X_F/X_{OH} values with decreasing MgO contents (Fig. 2; middle). This is interpreted as a volatile-saturated magma which has already experienced a large degree of volatile exsolution and Cl stripping from the melt, with increasing X_F/X_{OH} values because F is the only remaining volatile species in the melt for apatite to incorporate. These interpretations are supported by numerical modelling. Modelling results suggest that the two phonolites were stored at 150 MPa and 870-890°C in volatile-saturated conditions, and the phonotephrite was stored in a volatile-undersaturated state at 300 MPa and 1050°C. Ascent and injection of the phonotephrite into the phonolite portions of the reservoir, as evidenced by preserved magma mixing textures in eruptive deposits, may have induced volatile saturation and primary boiling in the phonotephrite, and consequently triggered eruption.

References

[1] Candela (1986) Chem Geol **57**, 289-301 [2] Humphreys et al (2021) EPSL **576**, 117-198 [3] Bryan (2006) J Petrol **47**, 1557-1589 [4] Gonzalez-Garcia et al. (2022) J Petrol **63**, 1-24

Fig. 2. Volatile compositions of apatite inclusions from phonolite 1 (top), phonolite 2 (middle) and the phonotephrite (bottom). Apatite MgO content (colour bar) is used as an index of fractionation to show evolutionary trends. Phonolite 1 apatites decrease sharply in X_{Cl}/X_{OH}, indicative of progressive volatile exsolution. Phonolite 2 apatites record low X_{Cl}/X_{OH} and increasing X_F/X_{OH}, suggesting increasing fractionation following prior volatile exsolution. The phonotephrite shows an increase in X_F/X_{OH} and X_{Cl}/X_{OH}, indicating that it remained volatile-undersaturated and became progressively volatile-enriched with fractionation.

Investigating the source of deformation-controlling fluids in the mid crustal Badcall shear zone, NW Scotland

M. Carpenter and S. Piazolo

School of Earth and Environment, University of Leeds, Leeds Edinburgh LS2 9JT, UK

Background

The presence of fluid is known to influence the strength of the Earth's crust, and how it deforms in response to stress. To build robust models of the earthquake cycle on crustal-scale faults, the source and pathways of any available is one of the variables we need to understand. Field and microstructural studies show that fluid influx was critical to the development of the mid-crustal, ductile Badcall shear zone where, with strain and proximity to the shear zone, hydration and quartz vein abundance increases and deformation mechanisms change [1]. It has been shown that the isotopic composition of oxygen can indicate the source of fluids in Earth's crust: meteoric water has $\delta^{18}O_{SMOW}$ < 0 ‰, while magmatic or metamorphic fluids typically have values from ~5 to 10 ‰, and metamorphic fluids associated with sedimentary rocks have higher values of >10 ‰ [2]. In this pilot study we use in-situ analysis of oxygen isotopes in quartz to 1) understand the source of the quartz-bearing fluids in Badcall shear zone, 2) to understand how these fluids interact with the host rock. We analyse distinct quartz populations in both quartzofeldspathic gneiss and amphibolite dyke, from both the wall rock, outside of the shear zone, and from the shear zone centre.

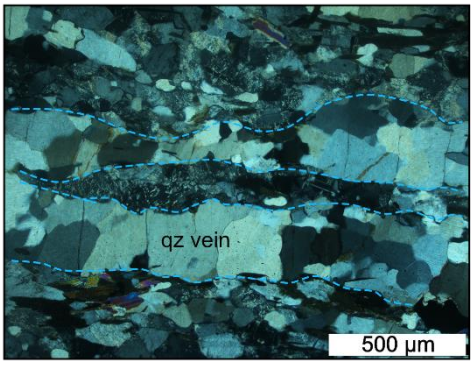

Fig. 1. Crossed-polars photomicrograph showing quartz vein in quartz-feldspar gneiss in the shear zone centre.

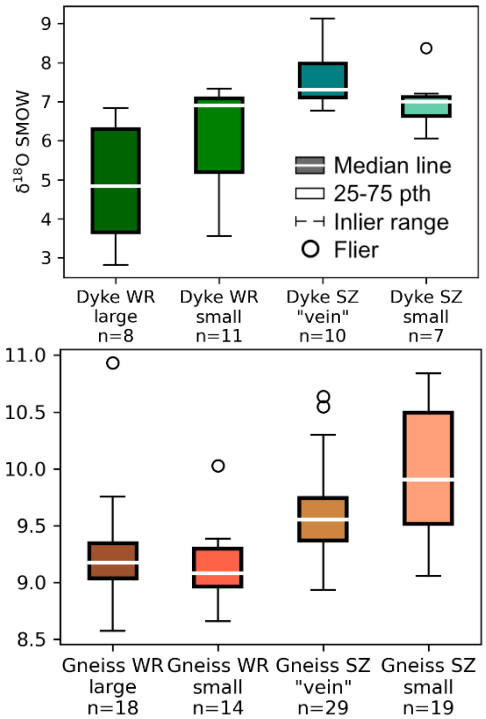

Fig. 2. Results of showing $\delta^{18}O$ in the high strain shear zone centre (SZ) compared to the undeformed wall rock (WR).

Results and Interpretation

We observe a clear difference in quartz $\delta^{18}O$ with rock type, with values between 3-9 in the dyke and 9-11 in the gneiss. In shear zone dyke, $\delta^{18}O$ is higher relative to the wall rock, with mean values of 7.4 and 5.6. Small quartz in the wall rock dyke trend towards the shear zone quartz. We interpret these to be the product of reactions that are driven by fluids related to the shear zone, that infiltrate and weaken the wall rock prior to deformation. In the gneiss the overall range in $\delta^{18}O$ values is much smaller but we do see a tentative trend similar to the dyke: average values are higher in the shear zone compared to the wall rock, with mean values of 9.75 and 9.1 respectively. The higher $\delta^{18}O$ quartz in the shear zone could mean that infiltrating fluids have a magmatic or metamorphic isotopic ratio, or that, as fluid reacts with the rock, it mixes with higher $\delta^{18}O$ sources (i.e. released from minerals during metamorphism). The results show there is a tentative isotopic change in $\delta^{18}O$ quartz signature associated with the shear zone, however, the data is not conclusive. Therefore, more extensive work will be needed in the future to better constrain the trends and thus the source and interaction of such fluids with the rock during contemporaneous metamorphism and deformation.

References

[1] Carpenter et al (2022) EGU22-13366 [2] Stenvall et al (2020) Geofluids **1**

Tracking magmatic changes prior to large explosive and effusive eruptions through volatile analyses in apatite and melt inclusions

M. Cassidy[1], M. Humphreys[2], V. Smith[3], D. Pyle[3], T. Mather[3], M. Stock[4], R. Brooker[5], P.Ruprecht[6]

[1]University of Birmingham, Birmingham, UK, [2]University of Durham, UK, [3]University of Oxford, UK, [4]Trinity College Dublin, Ireland, [5]University of Bristol, UK, [6]University of Nevada, Reno, USA

Background and rationale

Magmas that feed volcanic eruptions may undergo significant changes in dissolved volatile content and oxidation state in the lead up to activity. These changes have fundamental impacts on the explosivity of eruptions, and can be recorded the by crystals that grew in the lead up to eruption. In this study, we have analysed a suite of samples from Quizapu Volcano in Chile, where deposits from recent eruptions of contrasting eruptive style are preserved. We have determined the oxidation state of sulfur in the phosphate mineral apatite by micro-XANES and will combine these data with measurements of their volatile chemistry from SIMS and Electron probe analyses. Analysing apatite crystals that have been sealed from contact with the host melt at different times and trapped as inclusions within other minerals, enables changes in volatiles and oxidation state to be tracked during pre-eruptive magmatic evolution. Traditional methods used to measure volatiles (e.g. melt inclusions), provide an insight into only the shallowest processes related to ascent and degassing, but suffer post-entrapment problems, such as loss of volatiles to the vapour phase (e.g. CO2 in melt inclusion bubbles) and diffusive loss of H through the host crystal. A rapidly advancing approach is the use of apatite, a calcium phosphate mineral, which is less vulnerable to post-preservation volatile losses than melt inclusions. Apatite incorporates volatile species OH, Cl, F, S and C into its structure, meaning that important information regarding pre-eruptive volatile behaviour, can be retrieved thanks to recent analytical, experimental and theoretical advances[1,2].

The key process that can fundamentally change volatile behaviour during pre-eruptive magma evolution is magma mixing. The effect of magma mixing on the explosivity of an eruption is contested. Some studies suggest that mixing can trigger explosive volcanism, by introducing excess volatiles to the system and increasing the magma overpressure[3]. Other studies suggest that magma mixing adds heat, initiating changes in viscosity and volatile exsolution and therefore leading to effusive eruptions [4]. What is missing from this debate are data to show how volatiles behave before, during and after magma mixing, which these data aims to address.

Samples and Methodology

Quizapu volcano in Chile, has produced some of the largest eruptions in South America in the last two centuries, it is also an outstanding case study to study both magma mixing and the controls on eruptive style. Quizapu erupted effusively in 1846 and explosively in 1932, despite erupting the same volume of magma (4 - 7 km^3), and the same magmatic composition (dacite). Both the effusive and explosive eruptions show evidence for magma mixing in their eruptive products, yet they led to completely contrasting eruptive styles.

A set of melt inclusions and apatite crystals were analysed from Quizapu's volcano eruptive products from 1846 (effusive eruption) and 1932 (explosive eruption), along with their mixed end members. The rocks have been crushed, sieved, with apatites separated using density and magnetic methods in the Free University, Amsterdam. Apatite separates were mounted, ready for SEM and chemical analysis.

Glass standards used ranged from basaltic to rhyolitic and apatite standards from a block prepared and subsequently analysed from co-Is, Brooker, Humphreys and Smith. As well as microphenocrysts, apatite crystals found within multiple different mineral phases were sampled. The apatite analyses were analysed over two SIMS trips, separated by COVID. Initial SIMS data for these apatites (mid-October 2019) give OH values of 0.3 – 1.4% and CO2 values of 300 - 3000 ppm. The water fraction of these apatites ranges from 0.67 to 0.94. Volatile concentrations (H, C, F and Cl) and some trace

elements (Na, Mg, Si & Ti) were also determined directly in apatite by SIMS using a Cameca ims-4f instrument, following pre-existing protocols[1]. EMPA determination of Cl and F as well as some other major elements of the same crystals are yet to be analysed, but will provide a comparison for the halogen measurements here.

Results and preliminary interpretations

	H_2O (wt%)	CO_2 (wt%)	F (wt%)	Cl (wt%)
1846 Inclusions (n=22)	0.94	0.12	1.96	0.95
1846 mafic enclave inclusions (n=14)	0.64	0.04	1.89	1.09
1932 Inclusions (n=8)	1.06	0.11	1.90	1.02
1932 Terminal scoria inclusions (n=3)	1.20	0.15	2.14	1.21

Table 1. Volatile analyses of apatite inclusions within pyroxene phenocrysts for different units.

Apatite analyses will be combined and compared with Electron microprobe data on the same apatites, and stoichiometric calculations will enable proper comparisons between the different units. Despite this early stage of processing, initial results suggest differences in the volatile compositions between the explosive and effusive eruptions, and their source magmas (Table 1). More data about the evolution of the magmatic volatiles will come from an analysis of their other inclusions such as magnetite, plagioclase, their microphenocryst content, and a comparison with the volatiles from melt inclusions.

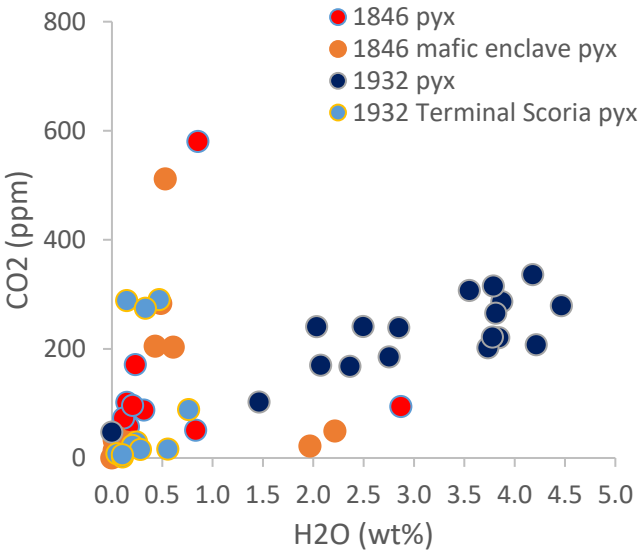

Fig. 1. Melt inclusion volatile contents for the different units. Blues indicate 1932 explosive eruptions and red and oranges the 1846 effusive eruption stages.

Figure 1 highlights the range of different volatile contents in the melt inclusions. The 1846 (effusive eruption), melt inclusions are mainly degassed, likely as a result of diffusive loss during slow cooling. Some mafic enclave inclusions display what might have been the primary melt water contents (~2 wt%). The terminal scoria unit at the end of the 1932 eruption also shows low CO_2 and water contents, both units show some anomalously higher CO_2 values. The main explosive unit of the 1932 eruption preserves high volatile contents (particularly water), up to 4.5 wt%, which may reflect the relative depth at which these magmas ascended and the speed of ascent to preserve their high water contents. Some processing to remove data that hit crystals, or hit the edge of the inclusion has been conducted, and these data will be analysed for any further post-entrapment crystallisation and mineral melt hygrometer calculations will allow for a comparison with data in Figure 1. The apatite and melt inclusion volatile data will be modelled thermodynamically to recreate initial bulk volatile contents for the magma, discern between second boiling and first boiling volatile evolution between the magma and co-existing vapour in the lead up to the eruptions[2].

References

[1] Riker et al. (2018) American Mineralogist **103**, 260–270
[2] Humphreys et al. (2021) Earth and Planetary Science Letters **576**, 117198.
[3] Murphy et al (1998) Geophysical Research Letters **25**, 3433–3436.
[4] Ruprecht and Bachmann (2010) Geology **38**, 919–922.

Volatile concentrations in melt inclusions from the Afro-Arabian LIP

D. Cirium[1], S. A. Gibson[1] & S. R. Passey[2]

[1] Department of Earth Sciences, University of Cambridge, CB2 3EQ, UK
[2] CASP, Cambridge, CB3 0UD, UK

Background

Volatile emissions from Large Igneous Provinces (LIPs) have been implicated in mass and minor extinction events, driven in part by short-term sulfur-mode cooling and long-term carbon-mode warming. The Afro-Arabian LIP is a compositionally-zoned and diachronously-emplaced tholeiitic continental flood basalt province overlain by alkaline shield volcanoes, with peak ages of 31-29 Ma in the north of the Ethiopian Highlands and 26-22 Ma to the south [1]. This protracted and pulsed eruption is contrary to LIP models wherein the bulk of flood volcanism occurs in a 1 Myr timeframe, and is perhaps linked to the muted climate response during Oligo-Miocene boundary, which records cooling and minor faunal turnover [2,3]. This is in strong contrast to other LIPs of comparable scale (e.g. the Deccan and Siberian Traps) which are associated with mass extinctions and long-term warming trends [4,5].

We aim to quantify pre-eruptive volatile contents from melt inclusion glasses in order to produce the first volatile budget for the Afro-Arabian LIP, and additionally investigate the spatial and temporal heterogeneity in volatile delivery to decipher the sources of these volatiles. We sample across multiple compositional provinces (high and very high Ti zones), age groups (31-29 Ma, 26-22 Ma), and rock types (tholeiitic and alkali basalts; picrites and meimichites; nephelinites) to encompass the geochemical diversity of the province (Figure 1). Principally, we focus on two area groups representative of the main phase of LIP flood volcanism (intermediate fraction silica-oversaturated melts from an asthenospheric plume source) and waning phase of LIP shield volcanism (low fraction silica-undersaturated melts sourced from deep carbonated ± phlogopite bearing mantle metasomes) with the expectation that these different mantle sources will impart distinct signatures on the volatile contents of their derivative magmas.

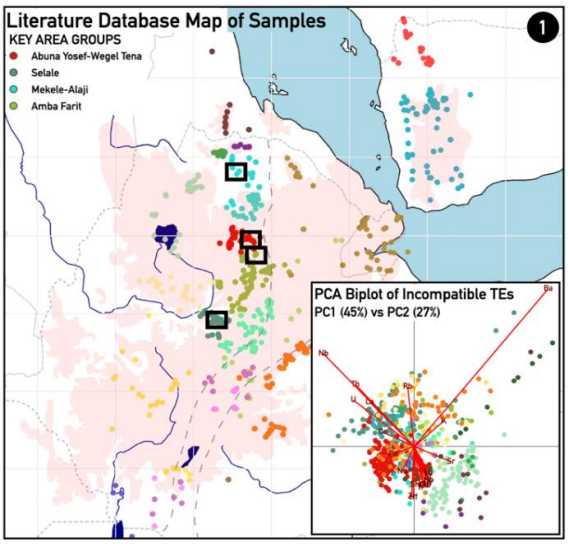

Fig. 1. Map of the Afro-Arabian LIP (pale red) and locations of literature samples. Samples from this study belong to four area groups (black boxes). Inset: PCA of primitive mantle normalised incompatible trace elements (TEs) shows a strong spatial control, reflecting heterogenous mantle and crustal sources. Samples from this study are found in the upper left and lower left quadrants.

Samples

Sixteen porphyritic samples were selected from which ~135 olivine and pyroxene hosted melt inclusions were prepared for analysis. Rare naturally glassy melt inclusions <30 um in diameter were typically found in clinopyroxenes and contained co-entrapped or daughter spinel crystals, the latter of which may concentrate volatiles by up to 10% in the melt. Vapour bubbles were also present but were either not analysed due to their small size or did not yield detectable concentrations of CO_2. Crystallised melt inclusions, typically >40 um in diameter and hosted in olivine, were rehomogenised using a Linkam1400 stage, with the resultant MIs bearing an exsolution vapour bubble and 1-2 co-entrapped spinels. Where possible, the vapour bubbles were analysed using Raman Spectroscopy, yielding up to 4500 ppm CO_2. Melt inclusions were then repolished and mounted in indium for the analysis of H_2O, CO_2, F, Cl, Li and B by SIMS.

Preliminary Results and Discussion

We present preliminary and uncorrected data normalised to 58% wt SiO_2. Work is ongoing to collect EPMA data for normalisation and post-entrapment crystallisation corrections, and LA-ICP-MS data for volatile-trace element systematics.

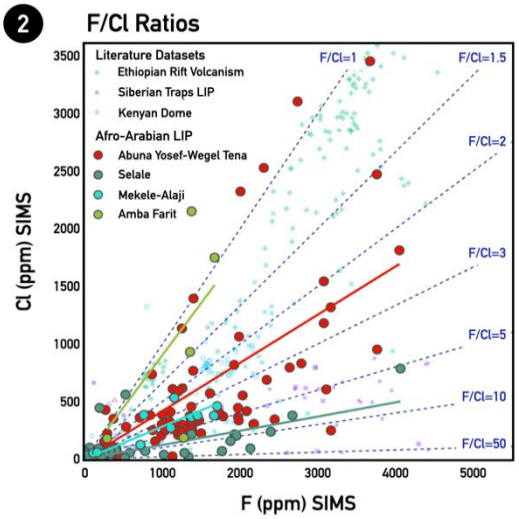

Fig. 2. F/Cl ratios from samples in this study and comparisons to literature datasets. Shield group samples from Selale have the highest F/Cl ratios (>5). Flood group samples from all other area groups have F/Cl <5, though these are still higher than values from recent rift volcanism products, likely reflecting both spatial and temporal variations in volatile sources.

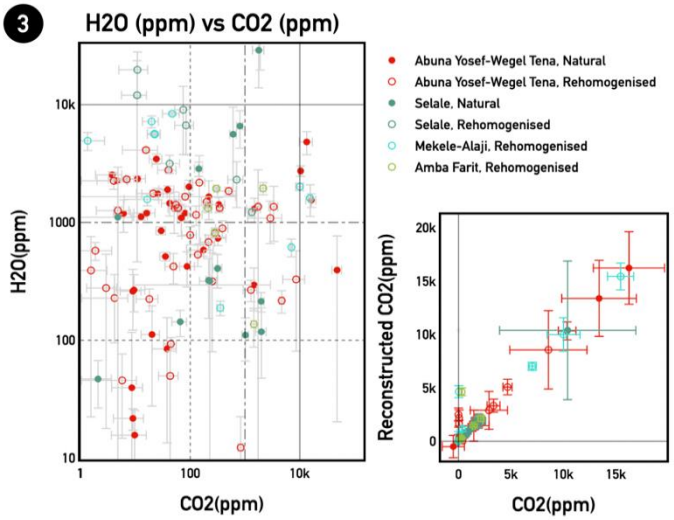

Fig. 3. CO_2 and H_2O data from naturally glassy and rehomogenised melt inclusions in this study. Several melt inclusions have CO_2 > 1 wt.%. Right: Reconstructed CO_2 contents from Raman Spectroscopy. CO_2 was only detectable in vapour bubbles where the corresponding glasses contained <1000 ppm CO_2.

Our halogen data (Figure 2) shows spatial variation in F/Cl ratios, with alkaline shield group samples exhibiting higher F/Cl ratios (>5) than flood basalt group samples (<5). We interpret these high F/Cl ratios to be inherited from a metasomatised mantle source containing F-hosting phases like phlogopite and apatite, and this is consistent with interpretations of source lithology from whole rock trace element and olivine minor element data. Flood basalt group samples show greater inter-sample variability, with two samples exhibiting F/Cl ratios of 1-2, similar to MIs from Quaternary rift volcanism studies in Ethiopia [6]. However, most flood basalt samples have higher F/Cl ratios than their modern-day counterparts, perhaps reflecting that in addition to spatial heterogeneity there is also a temporal element to the evolution of mantle sources over the last 40 Myr. This lends support to the hypothesis that there was early melting of easily fusible mantle metasomes post plume impingement [7], and that these metasomes were significant contributors to the volatile budgets of LIP magmas.

Our CO_2 data (Figure 3) shows that several melt inclusions from both naturally glassy and rehomogenised subsets contain in excess of 1 wt.% CO_2 (liable to c. ±20% changes post Si corrections). Most inclusions are, however, variably degassed, and therefore do not reflect pre-eruptive volatile concentrations. Further work will be done to obtain trace element LA-ICP-MS data to reconstruct these values using CO_2/Ba and CO_2/Nb systematics. Similar work will be undertaken to reconstruct pre-eruptive water contents using H_2O/Ce ratios, due to the effects of H loss during rehomogenisation.

References

[1] Passey et al (2018) CASP FBP Report 11 [2] Black & Gibson (2019) Elements, 15(5) 319–324 [3] Ernst (2014) Large Igneous Provinces [4] Black et al. (2018) Nature Geoscience 11(12) 949–954 [5] Callegaro et al (2023) Science Advances 9(40) [6] Iddon & Edmonds (2020) G^3 21(6) [7] Rooney et al. (2017) EPSL, 461 105–118.

The role of magmatic volatiles and saturation states in Plinian and inter-Plinian eruptions at Santorini, Greece

D.J. Colby[1*], M.C.S. Humphreys[1], C. Lormand[2], V.C. Smith[3], J.C.M. De Hoog[4], G. Vougioukalakis[5]

[1]Department of Earth Sciences, Durham University, Durham, DH1 3LE, UK
[2]Department of Earth Sciences, University of Geneva, UNIGE, Switzerland
[3]Research Laboratory for Archaeology and the History of Art, University of Oxford, Oxford OX1 3QY, UK
[4]EIMF, School of Geosciences, University of Edinburgh, Edinburgh, EH9 3FE, UK
[5]Hellenic Survey of Geology and Mineral Exploration, Aharne, Athens, Greece

Rational

Volatiles play a crucial role in the evolution of magmatic systems and in conditioning a magma reservoir for remobilization and eruption. Understanding the concentrations of volatiles in a melt, how these change with time, and the saturation state of the magma is essential for establishing the conditions necessary for explosive eruptions of varying magnitudes and probing the dynamics of complex mushy systems [1]. The common accessory mineral apatite [$Ca_5(PO_4)_3(F,Cl,OH)$] is a highly useful tool for assessing magmatic volatile contents, as halogens and OH are exchanged directly into the crystal structure, making them immune to the post-entrapment processes and diffusive loss that frequently affect analysis of melt inclusions [1]. Santorini (Greece) is an ideal location to investigate the role that volatiles play as a magmatic system changes between large-scale Plinian eruptions and smaller inter-Plinian events, as it has experienced numerous large-scale Plinian eruptions and significantly smaller mafic eruptions [2]. We investigate the changes in volatile concentrations and saturation state between these eruptions of different sizes through detailed analysis of apatite and the role volatiles play in the generation and mobilization of magma mush systems.

Materials and methods

We sampled pumice clasts from eight major Plinian eruptions at Santorini (Minoan, Cape Riva, Vourvoulos, Cape Thera, Middle Pumice, Lower Pumice 2, Lower Pumice 1 and Cape Therma 3) and four inter-Plinian eruptions (M8, M7, M6, M4 and M1). These samples were crushed, and clinopyroxene, orthopyroxene and Fe-Ti Oxides were picked. These were mounted, polished and analysed under a reflected light microscope to identify apatite inclusions. Heavy liquid separation was also carried out to collect apatite microphenocrysts. Both apatite microphenocrysts and inclusions were initially analysed for major-, minor- and volatile-element compositions using a JEOL 8600 electron microprobe at the Research Laboratory for Archaeology and the History of Art, University of Oxford. OH was initially estimated via stoichiometry. A subset of the apatites were directly analysed for H, C, F and Cl by secondary ion mass spectrometry (SIMS) using a Camec IMS 7f Geo instrument at the NERC Edinburgh Ion Microprobe Facility, University of Edinburgh.

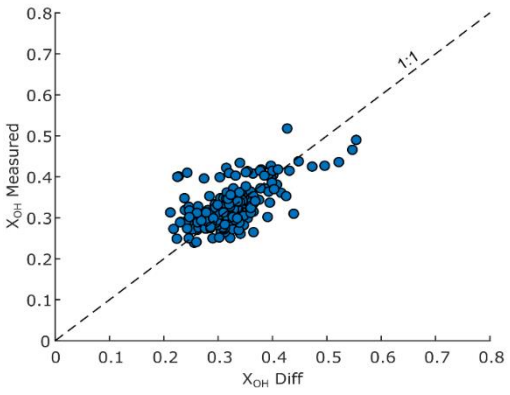

Fig. 1. Comparison of measured X_{OH} by SIMS and calculated X_{OH} by stoichiometry with 1:1 line. Data shows broad agreement but some deviation highlighting the need for SIMS work.

Results, implications and further work

Apatite from each eruptive unit has its unique apatite volatile signature. Apatites from eruptions at Santorini record fairly consistent F concentrations with the majority recording between 1.5- 2.5 wt.%. There are similar variations in Cl between 0.6 – 1.4 wt.% with some higher values up to 1.8 wt.%. OH was initially determined

via stoichiometry, and a subset underwent additional analysis under SIMS to directly measure H_2O. By comparing these two datasets, we show that they are in broad agreement (Figure 1). There is some deviation from the 1:1 line; however, this is not systematic across the dataset, making it challenging to apply a broad correction to our whole dataset. This highlights the need for SIMS to quantify OH in apatite accurately.

All eruptions show a similar linear evolutionary trend (Figure 2) with clear separation between eruptions in eruptive Cycle 1 and 2. However, the direction of this trend needs to be determined; therefore, MgO was used as a proxy for melt evolution. Using MgO as a tracer allows us to identify the direction of fractionation, which is towards increasing in X_{Cl}/X_{OH} with X_F/X_{OH}.

Using an apatite fractionation model [3], we calculate the initial volatile concentrations of the melts from each of these eruptions and the evolution of volatiles in the magmatic system throughout apatite crystallisation. We also investigate the saturation state (water saturated or undersaturated) by conducting modelling under both scenarios. Preliminary analysis indicates that the large-scale Minoan and Cape Riva eruptions were water-saturated; however, the caldera-forming eruptions of Lower Pumice 1 and Lower Pumice 2 are likely water-undersaturated. In addition, the smaller inter-Plinian eruptions were water undersaturated. This poses several further lines of investigation around the differences between magma accumulation and eruption triggering between the Plinian and inter-Plinian eruptions at Santorini and the dynamics of magma mush.

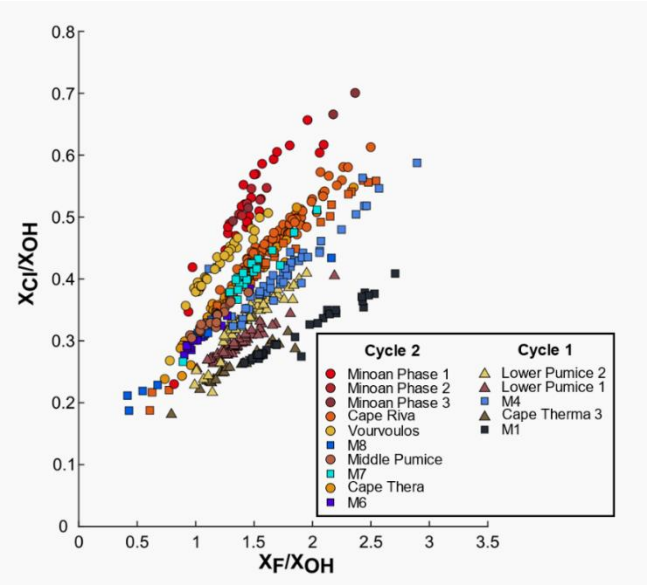

Fig. 2. Apatite volatile compositions for the different eruptions at Santorini. Each eruption has a distinct volatile trend and is increasing in X_{Cl}/X_{OH} with increasing X_F/X_{OH}.

References

[1] Humphreys et al. (2021) Earth and Planetary Science Letters **576**, 117198.
[2] Druitt et al. (2016) Journal of Petrology **57**(3) 461-494.
[3] Lormand et al. (2024) Lithos **480**, p.107623.

This work was developed during the Consolidator grant for the STEMMS project (STorage and Eruption of Mushy Magma Systems) awarded to PI M.C.S. Humphreys and supported by the European Research Council under the European Union's Horizon 2020 research and innovation programme [grant number 864923].

Exploring the volatile contents and trace elements of melt inclusions from Kombiu volcano, Papua New Guinea

M. Höhn, B. McCormick Kilbride & M. Hartley

Department of Earth and Environmental Science, University of Manchester, Manchester, M13 9PL, UK

Background and Objectives

Rabaul is an arc volcano on the eastern tip of the New Britain volcanic arc and has historically been the most active volcano in Papua New Guinea. Rabaul is capable of large volume, high intensity caldera-forming eruptions as well as low intensity but more frequent intra-caldera eruptions. Any eruption at Rabaul poses a serious risk to local communities. Rabaul exhibits clear evidence of recurrent mafic recharge and magma mixing, as demonstrated by the presence of mafic enclaves. Despite these observations, the chemical composition of the mafic recharge magma at Rabaul has been only loosely constrained using basaltic enclaves [1]. Although currently an independent edifice, Kombiu was a parasitic cone on the ancestral Rabaul volcano approximately 100 kyr ago [2]. This geological affinity suggests that the same magma plumbing system may feed both Kombiu and Rabaul, with Kombiu's predominantly basaltic and basaltic andesite compositions potentially representing the mafic recharge component of both volcanic systems.

We characterised the chemical composition, including volatile (H_2O, CO_2, SO_2, Cl, F) and trace element contents, of melt inclusions in Kombiu scoria, and correlate these data with melt inclusions in volcanic bombs from the 2014 eruption at Rabaul [3].

Results

We used the 7f-GEO instrument to measure H_2O, CO_2, F and selected trace elements in >50 naturally quenched, glassy olivine-hosted melt inclusions (MIs) and matrix glasses. Major elements, Cl and SO_2 were measured afterwards by electron probe microanalysis at the University of Manchester, UK. Post-entrapment crystallisation (PEC) corrections were carried out for all melt inclusions by adding the host mineral composition incrementally back into the melt inclusion until the equilibrium K_D value between melt and mineral was reached.

Olivine-hosted melt inclusions from the Kombiu scoria have a basaltic composition (46.1–50.4 wt% SiO2, mean 48.1 wt%) and are overall more primitive than olivine-hosted melt inclusions from volcanic bombs of the 2014 eruption at Rabaul (46.9–57.8 wt% SiO2, mean 52.8 wt%) (Fig. 1). Kombiu melt inclusions show a wide range in H_2O contents with maximum H_2O concentrations of ca. 2.8 wt% which is similar to the maximum H_2O contents shown by the Rabaul melt inclusions. Furthermore, both the Kombiu and Rabaul melt inclusions follow similar CO_2 degassing paths (Fig. 2a). The Kombiu melt inclusions predominantly centre around 4500 ppm SO_2 and have therefore overall around 1000–1500 ppm more SO_2 than the Rabaul melt inclusions (Fig. 2b). Overall, the Kombiu and Rabaul melt inclusions show remarkably similar volatile contents supporting the interpretation that both volcanic systems share a comparable magmatic evolution.

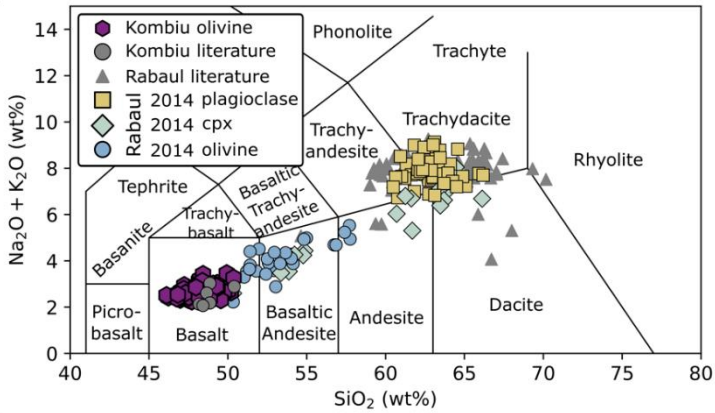

Fig. 1. TAS diagram comparing melt inclusions from the Kombiu scoria with those of volcanic bombs from the 2014 eruption of Rabaul [3] and literature data [4, 5]. Shown here are PEC corrected data.

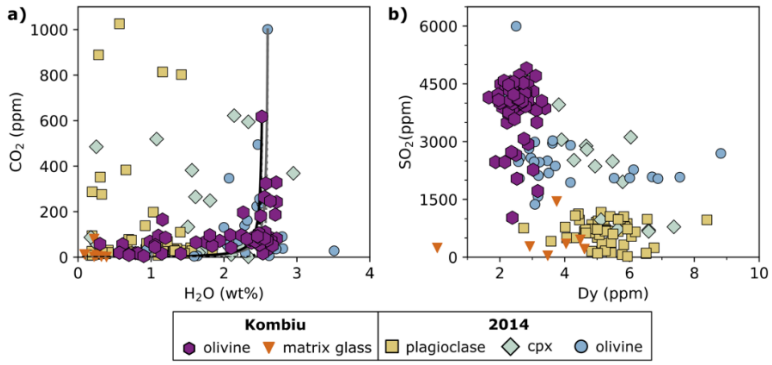

Fig. 2. Comparison of a) CO_2 vs H_2O and b) Dy vs SO_2 contents melt inclusions from the Kombiu scoria and those from volcanic bombs from the 2014 eruption of Rabaul [3]. Closed- and open-system degassing paths are shown with bold and dashed lines [5]. Symbols and colours as in Fig. 1. Shown here is PEC corrected data.

The presence of elevated LILE/HFSE ratios (e.g. Sr/Nd) in the Kombiu and Rabaul melt inclusions and generally elevated ratios of fluid-mobile against fluid-immobile elements indicates that both the Kombiu and Rabaul magmas are enriched in slab-derived fluids (Fig. 3a). On the other hand, low Th/Yb ratios in both the Kombiu and Rabaul melt inclusions indicates only minor sediment addition from the slab. A plot of Th/La vs. Sm/La can be used to assess the composition of subducting slab sediments and the degree of depletion of the mantle source (Fig. 3b). The sediment component for the New Britain subduction zone is loosely constraint by an average sediment composition from the Solomon Sea with a Th/La ratio of ~0.175 and New Britain lavas form an array between their estimated mantle source and the subducted sediment. The Rabaul and Kombiu melt inclusions lie on an array between sediment and mantle source that indicates mantle Sm/La ratios of ~0.75. This suggests a relatively enriched mantle source for the Rabaul and Kombiu magmas compared to the remainder of the New Britain arc. We propose two possible explanations for this. First, if the highly depleted nature of the New Britain mantle source is related to melt extraction in the nearby Manus spreading centre, then the Rabaul mantle wedge may have been somewhat less affected. Alternatively, Rabaul's mantle wedge might be not only less depleted but actually enriched, which could stem from the introduction of recycled slab components during an earlier episode of subduction, specifically the south-westward subduction of the Pacific plate along the now-inactive Manus-Kilinailau margin, which lies the northeast of Rabaul. Subduction along this margin is estimated to have ended in the Miocene.

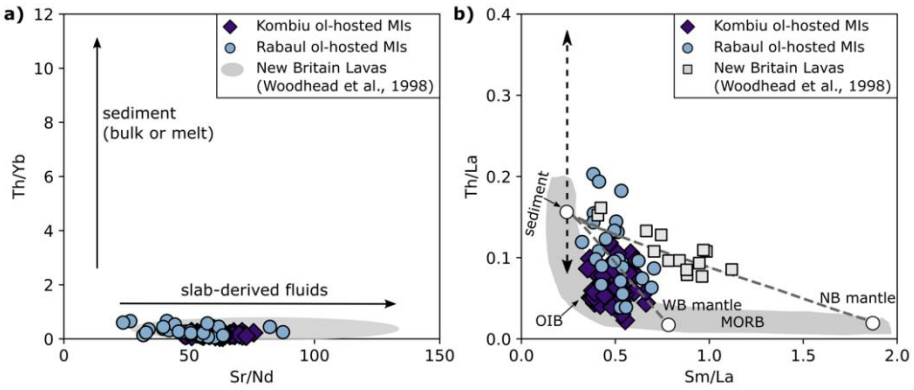

Fig. 3. Comparison of a) Th/Yb vs Sr/Nd and b) Th/La vs Sm/La contents in melt inclusions from the Kombiu scoria with those from volcanic bombs from the 2014 eruption of Rabaul [3] and lavas from the New Britain volcanic arc [6]. Shown here is PEC corrected data. NB = New Britain, WB = Western Bismarck.

References

[1] Fabbro G et al. (2020) J Volcanol Geotherm Res 393:106810 [2] McKee C et al. (2016) Bull. Volcanol. 78 [3] Höhn et al. (in prep) [4] Roggensack K et al. (1996) Science 273:490-493 [5] Bouvet de Maisonneuve C et al. (2015) Geol Soc London Spec Publ 442:17-39 [6] Woodhead J (1998) J. Petrol. 39:1641–1668

Volcanic sulfur emissions from magma source to ice core archive: the case of the 1783 Laki eruption

W. Hutchison[1], F. Brouillet[1], A. Burke[1], P. Sugden[1], M. Hartley[2], D. Neave[2], Z. Taracsák[3]

[1]School of Earth and Environmental Sciences, University of St Andrews
[2]Department of Earth and Environmental Sciences, University of Manchester
[3]Department of Earth Sciences, University of Cambridge

Background and rationale

Polar ice caps preserve exquisite records of volcanism on Earth because they capture sulfate aerosol fallout from major eruptions. Recent advances in ice core analysis have greatly energized this field, and one of the key developments is the analysis of sulfur (S) isotopes in ice core sulfate. These analyses provide exceptionally high-time-resolution (bi-monthly) isotopic records of volcanic plume fallout and encode detailed information about eruption source, style and plume evolution which could be used to determine climate impact. However, though the technique has immense potential, the processes that generate these unique isotopic signals remain poorly constrained. For example, we do not know if isotope fractionation dominantly occurs in the magmatic system, during eruptive degassing or subsequent atmospheric processing (Fig. 1). The key issue is that no study has carefully assessed S isotope evolution from eruptive source to ice sheet deposition.

We aim to address this issue by generating a detailed understanding of volcanic S isotopes at source and marrying these to state-of-the-art ice core isotope records of plume fallout. Our focus is the massive 1783 Laki eruption in Iceland which represents the largest ice core sulfate peak in Greenland over the last 2500 years (Fig. 1a). Our new ice core S isotope record (Fig. 1b) reveals two key features. Firstly, individual S isotope measurements ($\delta^{34}S$) reveal a time evolving signal, showing an initial decrease from background marine sulfate values of 8 ‰, to very negative values of –5 ‰ at the start of the S deposition, before rapidly switching to positive values of 2–4 ‰ in the middle and end of the S peak. Secondly, when we calculate the total S isotope value for the entire peak ($\delta^{34}S_{\Sigma fallout}$), by summing individual $\delta^{34}S$ contributions based on concentration, we obtain a value of ~0.8 ‰ (Fig. 1b).

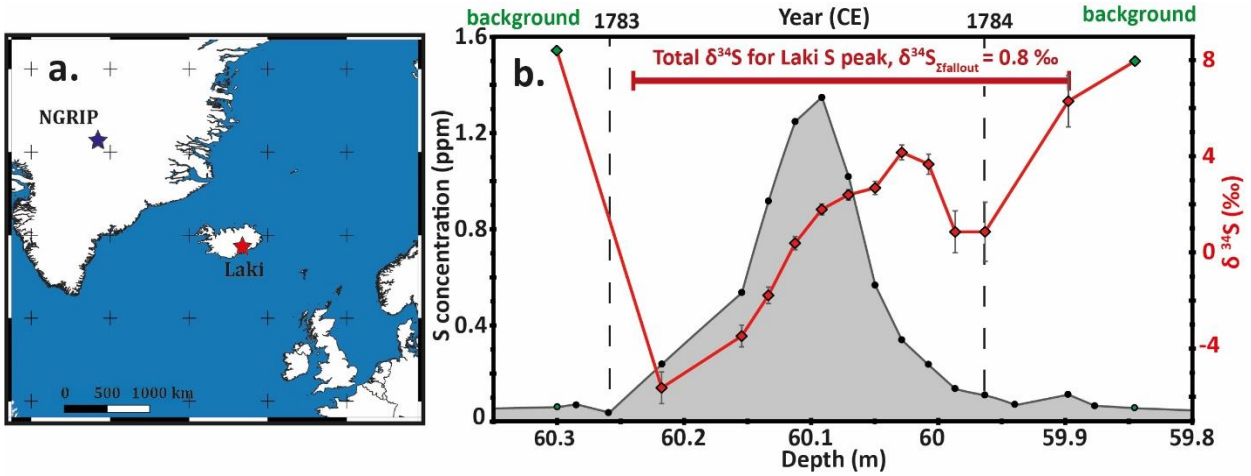

Fig. 1. Map (a) showing the location of the Laki fissure eruption and the NGRIP ice core which we have used to develop a new $\delta^{34}S$ record of plume fallout (b). $\delta^{34}S$ of individual samples are shown by red diamonds. Background samples, before and after the eruption, are shown as green symbols. The total S isotope value for the entire peak ($\delta^{34}S_{\Sigma fallout}$) is calculated by summing $\delta^{34}S$ of individual samples (weighted by their concentration).

SIMS data

The main objective of our SIMS project is to determine the initial $\delta^{34}S$ of the Laki melt (prior to magmatic degassing) and use isotopic mass balance to quantify $\delta^{34}S$ of the corresponding gas phase

($\delta^{34}S_{\sum gas}$). To achieve this, we analysed $\delta^{34}S$ and volatile concentrations in a suite of melt inclusions and matrix glasses from Laki tephra. Crucially, we seek to test whether the bulk gas signature, $\delta^{34}S_{\sum gas} \approx \delta^{34}S_{\sum fallout}$. If this assumption holds, it will demonstrate that we can use ice core records to constrain the initial $\delta^{34}S$ of the plume. This is important because we know that different volcanic systems have variable $\delta^{34}S_{gas}$ (depending on oxidation state and magma source), and so if successful it would provide a new approach for discriminating different eruption sources (e.g. arc vs. rift eruptions).

We measured the volatile content (H_2O, CO_2, F, S, Cl) and $\delta^{34}S$ of 34 (mainly olivine) melt inclusions and 13 matrix glasses using the Cameca IMS-1270 instrument (Fig. 2). We found that the melt inclusions display high, but variable S contents, between 700–1900 ppm but with most of the data between 1600 and 1900 ppm. Matrix glasses had much lower S contents (400-600 ppm). Melt inclusion $\delta^{34}S$ was mainly between –1 and +1 ‰, while matrix glass $\delta^{34}S$ showed values between –4 and 0 ‰. The lower S contents of the matrix glasses are consistent with magmatic degassing (i.e. where melt S is partitioned into SO_2 gas) and an interesting observation is that some of the most primitive olivines (those with forsterite, Fo, contents of 86) display intermediate S contents and a range of $\delta^{34}S$ (between –1 and +1 ‰).

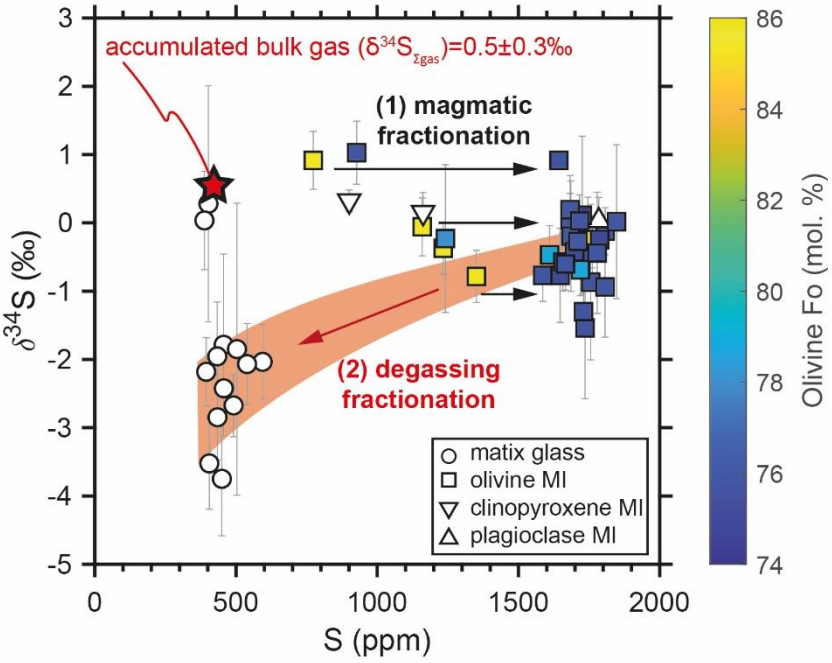

Fig. 2. Sulfur concentration versus $\delta^{34}S$ for the Laki eruption materials. Symbols correspond to matrix glass or melt inclusion (MI) analyses. For the olivine hosted melt inclusions the symbols colours reflect their forsterite, Fo, contents (those with highest Fo, yellow colours, are the most primitive). The two main trends in our data are linked to magmatic fractionation (black arrows) and degassing (red arrow). The $\delta^{34}S$of the accumulated gas phase (i.e. the $\delta^{34}S$ of gas emitted by the Laki eruption) is shown by the red star and is based on our mass balance modelling.

Our interpretation is that there are two main trends in our data (labelled 1 and 2 in Fig. 2). Prior to magmatic degassing S behaves as an incompatible element, i.e. we see an increase in melt sulfur content as the olivine forsterite content decreases. As this process takes place as at high magmatic temperatures there is no detectable change in melt $\delta^{34}S$, and so a horizontal trend is shown in Figure 2. The second trend is magmatic degassing and using isotopic fractionation factors and an oxygen fugacity (fO_2) set at the QFM±1 buffer (consistent with petrological constraints) we can reproduce the decreasing $\delta^{34}S$ between the melt inclusions and the matrix glasses.

Our modelling also allows us to reconstruct the $\delta^{34}S$ of the accumulated gas phases ($\delta^{34}S_{\sum gas}$). This value is ~0.5 ‰ (Fig. 2). It is very close to the ice core value ($\delta^{34}S_{\sum fallout}$) of ~0.5 ‰ and thus, $\delta^{34}S_{\sum gas} \approx \delta^{34}S_{\sum fallout}$. Given that the difference between magmatic gases from arc and rift settings is on the order of +2 to +5 ‰ this indicates that the $\delta^{34}S$ of ice core fallout could be used to differentiate between these different eruption settings. This is an important finding; because the vast majority of S peaks in the polar ice cores have yet to be linked to a known volcano, these results demonstrate that S isotopes of ice core sulfate have the power to reveal the geotectonic setting of unidentified volcanic events and thus, significantly improve our understanding of Earth's volcanic record.

Hydrogen in rutile

M. Lueder, J. Hermann & D. Rubatto

Institute of Geological Sciences, University of Bern, Baltzerstrasse 1+3, 3012 Bern, Switzerland

Rationale

Rutile is a very common accessory mineral in high-grade metamorphic rocks related to modern-style cold subduction, and is very stable during sedimentary processes, making it a valuable petrogenetic indicator in metamorphic and detrital settings. Hydrogen contents in rutile are partially pressure dependent, and combined with other trace element contents, can be used to identify rutile formed under modern-style cold subduction condition [1]. Therefore, detrital rutile can be used to trace cold subduction conditions in the Precambrian sedimentary record.

H_2O in rutile is typically measured by Fourier Transform Infrared (FTIR) spectroscopy, which requires the use of double polished thick-sections or single grains. This makes sample preparation tedious, especially for detrital grains used for provenance studies. Secondary Ion Mass Spectrometry (SIMS) offers a promising alternative with a more straightforward workflow and better spatial resolution, which is beneficial given the heterogeneity of H_2O in rutile [1].

Contrary to FTIR, SIMS requires well-characterized reference materials, which do not yet exist. Since no natural rutile with homogeneous H_2O content has been identified, we evaluate synthetic, hydrated rutile as potential reference materials.

Approach

We performed preliminary tests on hydrated, pure and trace element doped, synthetic rutile to evaluate these materials as potential H-in-rutile reference material. The synthetic rutile was hydrated using piston cylinder experiments at different pressure, temperature and oxygen fugacity conditions, to obtain rutile with different H_2O content. Representative pieces of each run product were analysed by FTIR to evaluate the H_2O contents and homogeneity. All materials were hydrated and showed homogeneous H_2O contents [2]. The same pieces that were measured by FTIR were then used for SIMS measurements.

Results

The obtained H counts for each synthetic rutile grains are homogeneous and H counts for selected grains are consistent across different sessions within two measurement days. However, no direct correlation between H counts from SIMS measurements and H_2O contents from FTIR analysis were observed (Fig. 1). No data points fall into the 1sigma uncertainty envelope on the regression line and the R^2 value is 0.884.

The cause of the observed scatter is not yet clear. As FTIR-H_2O contents and SIMS-H counts are consistent for each individual grain, intrinsic heterogeneities can be ruled out as cause. As H counts are consistent across two days, drifts over time are also not the cause of the misfits. As Fe contents are generally low (< 10 µg/g), Fe cannot have a significant influence on the results.

This leaves orientation effects as the most likely cause for the scatter. All grains are cut approximately perpendicular to the a-axis. However, the orientation of the rutile grain relative to the incoming beam was not constrained. Thus, further tests are necessary to evaluate the potential orientation effects and find a suitable measurement approach for hydrogen in rutile by SIMS.

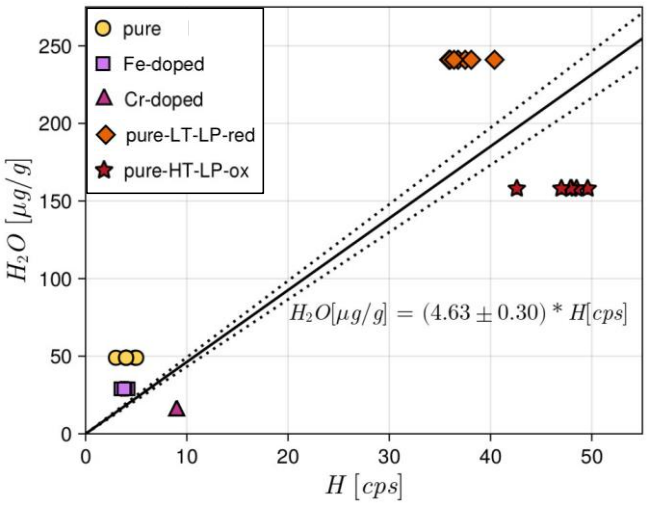

Fig. 1. Calibration line for evaluated potential reference material. Hydrogen counts from SIMS analysis vs. H_2O contents from FTIR measurements. The regression line is given with a 1sigma uncertainty envelope. The R^2 value of the regression is 0.884.

References

[1] M. Lueder et al. (2024) Contributions to Mineralogy and Petrology **179**:26
[2] M. Lueder et al. (2024) Swiss Geoscience Meeting, Basel

Unlocking the Carbon budget of the Earth

O. Shorttle[1,2], J. Shea[1] & J. Maclennan[1]

[1]Department of Earth Sciences, University of Cambridge, Cambridge CB2 3EQ, UK
[2]Institute of Astronomy, University of Cambridge, Cambridge CB3 0HA, UK

Scientific Report

Our project is investigating the origin of carbon in the Earth's mantle. The study is focussed on basaltic samples that tap into various mantle reservoirs that may have a different origin of their carbon. As carbon degasses so readily from basalts, it is critical that we are able to compare carbon concentrations to that of trace elements with similar compatibility during mantle melting, such that we can separate the effects of degassing from variable degrees of melting. We also targeted olivine-hosted melt inclusions to mitigate the effect of degassing as far as possible, and see deeper into the magmatic system.

Trace element analyses were carried out using the CAMECA ims 7f-Geo. This instrument provided excellent volatile and trace element data, which are included below in Figure 1.

The project also aimed to develop carbon isotopes in basaltic melt inclusions as an independent means of correcting for carbon loss by degassing. We experimented with implementing this technique on the 1270. Using the instrument in mono-collection mode provided key experience of the challenges and method developments required to obtain high-precision data. Upgrades to sample preparation equipment, notably the ion-mill, used as part of this work also demonstrated significant reduction in surface contamination for volatile analyses. This is currently world leading and is an approach other labs are now adopting.

The carbon isotope techniques started at the NERC-EIMF were built on for our first methods publication arising from this work [1] and subsequent science application [2], as well as several conferences [3-5].

The analyses and methods developed out of this work open up an important new tool for igneous petrology. This is reflected in the independent research fellowship Shea has written to extend and apply these developments, aiming to use the ims-1300HR once fully commissioned to bring this new method to the UK.

References

[1] Shea et al (accepted) Improved Precision and Reference Materials for Stable Carbon isotope Analysis in Basaltic Glasses using Secondary Ion Mass Spectrometry. Geostandards and Geoanalytical Research.
[2] Shea et al. (in preparation). Heavy carbon in Iceland's primordial reservior.
[3] Shea et al. (2024) Enhanced precision on *in situ* measurements of stable carbon isotope ratios in basaltic glasses (abstract). AGU24, Washington D.C.
[4] Shea et al. (2025). Heavy carbon in Iceland's primordial reservoir (abstract). Goldschmidt 2025. Prague, Czech Republic
[5] Shea et al. (2025) Fingerprinting Earth's mantle carbon reservoirs (abstract). VMSG-MDSG 2025 Joint Meeting. Dublin, Ireland.

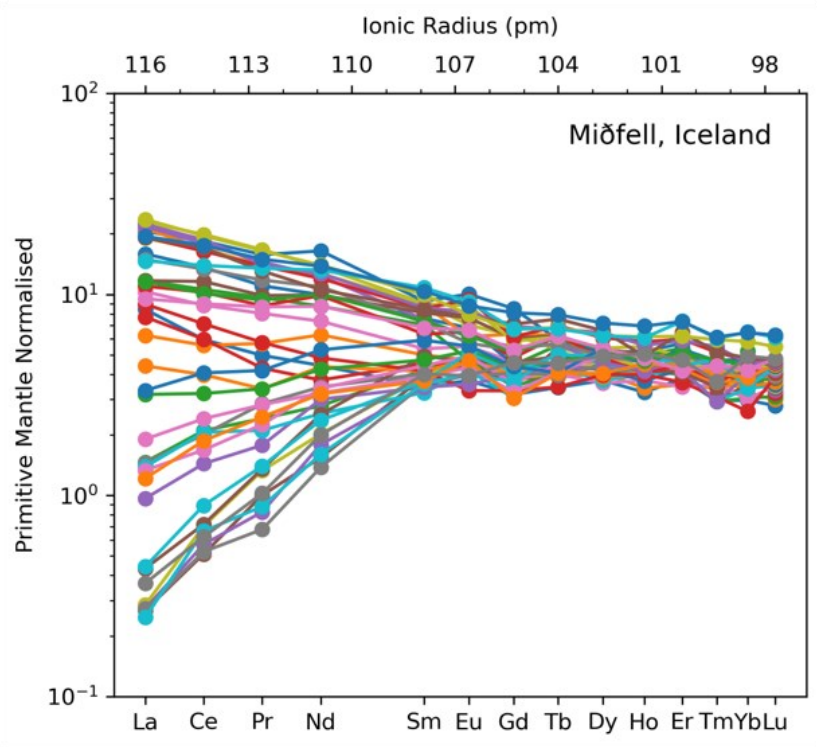

Fig. 1. Rare Earth Element (REE) variation diagram for Miðfell, Iceland, based on data collected at the IMF.

Volatile evolution of silicic magmatic systems in the Central Main Ethiopian Rift; insights from melt inclusions and apatite crystals of Tullu Moye and Boset volcanoes

A. Z. Tadesse[1, 2], V. C. Smith[3], K. Fontijn[4], M. C. S. Humphreys[5], T. A. Mather[2] & D. M. Pyle[2]

[1]Department of Earth Sciences, University of Oxford, UK. [2]School of Earth Sciences, Addis Ababa University, Ethiopia. [3]School of Archaeology, University of Oxford, UK. [4]Department of Geosciences, Environment and Society, Université Libre de Bruxelles, Belgium. [5]Department of Earth Sciences, Durham University, UK.

Background

Volatiles (H_2O, CO_2, S, F and Cl) are important constituents of most magmas, and have a major influence on magma evolution and eruption dynamics. The exsolution and expansion of volatile species drive volcanic eruptions, while their pre-eruptive behavior plays a key role in controlling eruption style [1]. Understanding volatile systematics during late-stage magma storage and the onset of magma ascent is therefore essential for identifying eruption-triggering processes and recognizing surface warning signs of imminent eruptions. Given the fundamental role of volatiles in volcanic activity, quantifying their pre-eruptive concentrations remains a priority in volcanological research.

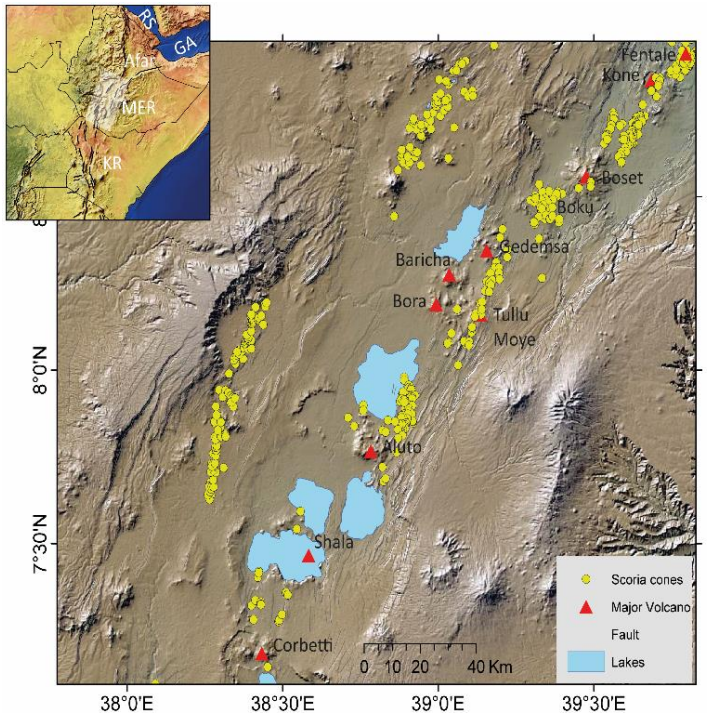

Fig. 1. Overview of the Main Ethiopian Rift showing the spatial distribution of the Holocene silicic and basaltic eruptive centres.

This study aims to quantify and improve our understanding of volcanic volatiles in silicic magma using melt inclusion and apatite analyses. We focus on Tullu Moye and Boset volcanoes, located in the central sector of the Main Ethiopian Rift (MER). The MER is a mature continental rift where the continental lithosphere is tearing apart (Fig. 1). It hosts more than a dozen active volcanoes, including Tullu Moye and Boset, which are likely to erupt again in the future. However, the volatile content of MER magmas remain poorly constrained. While a few studies have examined pre-eruptive dissolved volatiles in MER volcanoes using melt inclusion analysis [2], inclusions are susceptible to diffusive volatile loss and post-entrapment crystallization of the host mineral (e.g., [3]). To address these limitations, this study seeks to robustly quantify volatile evolution through a combined approach using analysis of both melt inclusions and apatite crystal.

Samples

Tullu Moye and Boset volcanoes are covered by young volcanic products. Tullu Moye has experienced at least two explosive eruptions in the past, while Boset has had six, with the two oldest eruptions from the Boset-Bericha volcanic centre. For this study, we targeted comendite deposits for volatile analysis: YTMP and OTMP from Tullu Moye and depositis #5 and #6 from Boset-Bericha. A total of

twelve samples were selected, with ten from Tullu Moye and two from Boset-Bericha, collected from different locations and eruption events. To prepare crystal grain mounts, fresh pumice clasts were manually crushed, dry-sieved, and individual clinopyroxene crystals were handpicked. The recovered mineral grains were cold-mounted in EpoFix resin rings and polished to achieve a flat, optically clear surface. Prior to the SIMS analysis, phenocrysts were initially inspected using reflected microscope and scanning electron microscope at the Department of Earth Sciences, University of Oxford. Subsequent geochemical analyses were conducted using an electron microprobe (EMPA) to quantify major elements (Si, Al, Na, Mg, Ca, K, Ti, Mn, P, La, Ce, Fe and Mn) and volatiles (F, Cl, S) in both the apatite phase and melt inclusions. Since conventional electron microbeam techniques are inadequate for precise characterization of light elements such as H and C, we scheduled SIMS analysis for 11-15 November, 2024 at the NERC EIMF facility. At EIMF, we analysed P, Ca, Mg, F, Cl, C, and H of 45 apatite inclusions, and Si, Mg, F, Cl, C, and H of 32 melt inclusions hosted in clinopyroxene from three samples. We are now in the final stage of data processing and are correlating the SIMS results with the EMPA dataset. Everything appears to be progressing well, and we are planning to write up a manuscript over the summer.

Result and implication

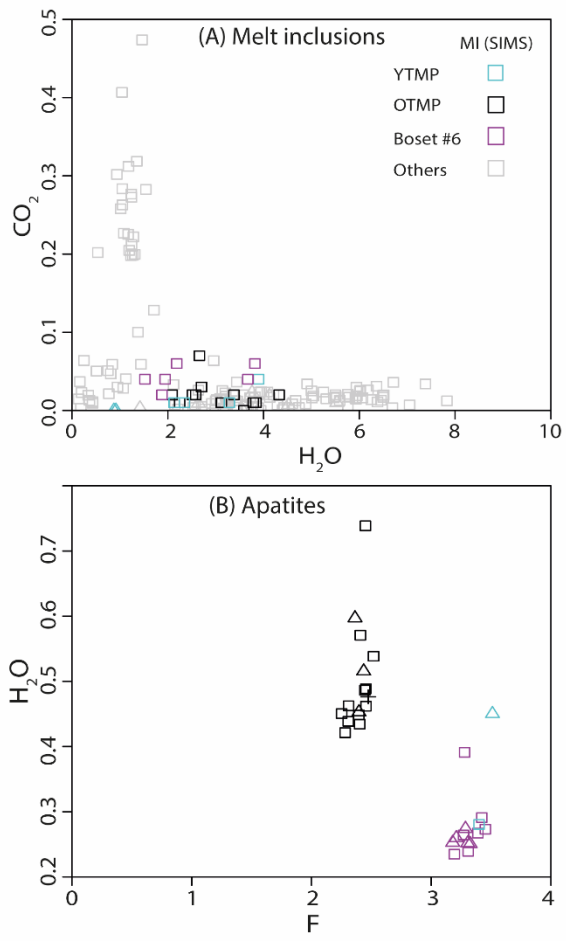

The analysis result reveals that apatite crystals from Tullu Moye and Boset volcanoes are predominantly fluorapatite, containing approximately 0.1-0.8 wt% Cl. Minor and rare earth elements such as FeO, MgO, MnO, La_2O_3 and Ce_2O_3 are also present in variable concentrations. Apatites from the older Tullu Moye (OTMP) show significant compositional variations, particularly in trace elements (e.g., MgO, MnO) and volatile species (Cl, F, H_2O). The volatile evolution trend further indicates distinct lineages for older Tullu Moye eruptions compared to more recent ones and the Boset-Bericha deposits. However, this compositional disparity is not reflected in the melt inclusion dataset (Fig. 2). All analyzed melt inclusions are compositionally peralkaline and comenditic, with Cl and H_2O as the only detectable volatiles. Since all analyzed melt inclusions are glassy, their volatile depletion may suggests post-entrapment degassing, which likely affected their ability to preserve original volatile contents. Consequently, slight discrepancies between the apatite and melt inclusion analyses may arise due to difference in volatile retention.

Fig. 2. Binary plots of (a) melt inclusion (MI), and (b) apatite compositions.

References

[1] Edmonds M (2008) *Philosophical Transactions of the Royal Society*, 366, 4559-4579.
[2] Iddon F & Edmonds M (2020) *Geochem. Geophys. Geosyst*. 21.
[3] Moore L R et al (2015) *Am Min*, 100, 806-823.

Sulphur cycling at subduction zones: insights from the Mariana and Tonga Arcs (western Pacific Ocean)

Z. Taracsák[1,2], T.A Mather[1], T. Plank[3], S. Ding[3,4], A Peccia[3], A. Auippa[5] & D.M. Pyle[1]

[1]Department of Earth Sciences, University of Oxford, Oxford OX1 3AN, UK
[2]Department of Earth Sciences, University of Cambridge, Cambridge CB2 3EQ, UK
[3]Lamont-Doherty Earth Observatory, Columbia University, Palisades NY 16094, New York, USA
4 Department of Geological Sciences, University of Florida, Gainesville, FL 32611, Florida USA
[4]DiSTeM, University of Palermo, 90123 Palermo, Italy

Background and Motivation

The Tonga and Mariana arcs in the western Pacific are located above the coldest subduction zones globally, where Mesozoic oceanic crust and variable amounts of sediment subduct today. Compared to our previous study localities (Aleutians, Central America) investigated as part of the NSFGEO-NERC grant "Sulphur cycling in subduction zones", Tonga and Mariana volcanics contain less sulphur (<3000 µg/g) but are comparatively oxidised at FMQ+1 to FMQ+3 [1,2]. To uncover the origin of sulphur and its relationship to redox and other slab tracers, we analysed sulphur isotopes ($\delta^{34}S$), volatiles, and trace elements from melt inclusions (MIs) containing variable amount of S to investigate the effects of degassing vs. source processes on $\delta^{34}S$ ratios.

Interlaboratory comparison of standards

Due to instrument downtime on the IMS-1270 in 2023, followed by delays caused by restricted access to the facility due to RAAC-related closure, we opted to carry out our S isotope analyses at the Woods Hole Oceanographic Institute (WHOI) SIMS facility in Massachusetts. This allowed us to carry out a comprehensive, inter-laboratory comparison on the sulphur isotope standards used in the two facilities. At WHOI, we used a different analytical setup compared to our past analyses in Edinburgh, which utilised a triple detector setup to collect $^{30}Si^-$, $^{32}S^-$, and $^{34}S^-$ ions simultaneously. We observed no instrumental mass fractionation (IMF) using the WHOI setup as a function of glass S content, in contrast to data collected in Edinburgh on the same standards (Figure 1A). We reanalysed a subset of unknowns at WHOI that we measured in Edinburgh in 2022 and found that after correcting the Edinburgh data for the S-content dependent IMF, we obtain reasonable agreement (within <1.5‰) between data collected at the two laboratories (Figure 1B).

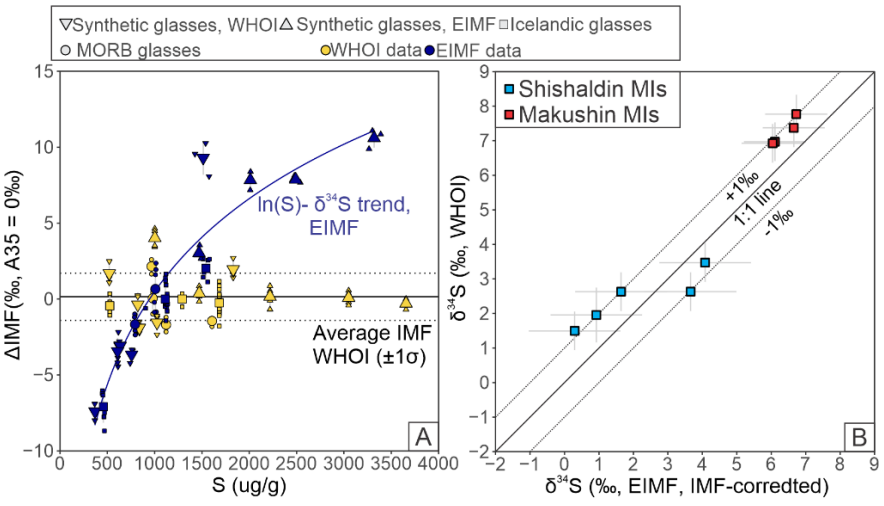

Fig. 1. (A) Instrumental mass fractionation (expressed in ‰, anchored to Icelandic glass standard A35 at 0‰) measured from various standards at EIMF (blue) and WHOI (yellow) plotted against glass sulphur content. Smaller symbols are individual analyses, while larger symbols are averages. (B) unknown data from Shishaldin and Makushin volcanoes (Aleutian Islands) that were analysed at EIMF in 2022 and WHOI in 2024. EIMF data were corrected for IMF using a ln(S) regression, after which the datasets agree within uncertainty. Error bars are 1σ. Calibration errors estimated using data from (A) are ±1‰ for EIMF and ±0.7‰ for WHOI (1σ).

After analyses of S isotopes at WHOI, we carried out volatile (H, C, F, Cl) and trace element (Li, B) analyses at EIMF using the IMS-7fgeo instrument in May 2024.

Results and discussion

Marianas and Tonga volcanic glasses have $\delta^{34}S$ values between 0 and +11‰, overlapping with data collected from the Aleutian and Central American arcs (-1 to +9‰). We estimate that undegassed melt $\delta^{34}S$ values for the seven studied localities are between +1 and +3‰, which also overlap with previous estimates from Central America and the Aleutian Islands (+1 to +5‰). Considering the extreme variability between thermal parameter [3] and sedimentary inputs (with highly variable $\delta^{34}S$) to these arcs, the narrow $\delta^{34}S$ range of arc magmas globally likely points to a common source/common process that controls their $\delta^{34}S$ compositions. Although Cl and F are correlated in several volcanic suites (Fig. 2C,D), we find no correlations between halogens, magma redox or undegassed $\delta^{34}S$ values. A possible scenario that can explain the narrow range of arc magma $\delta^{34}S$ values is that the oceanic crust provides much of the slab derived sulphur in arcs, which undergoes isotope fractionation during slab devolatilisation, as suggested by recent thermodynamic models [4].

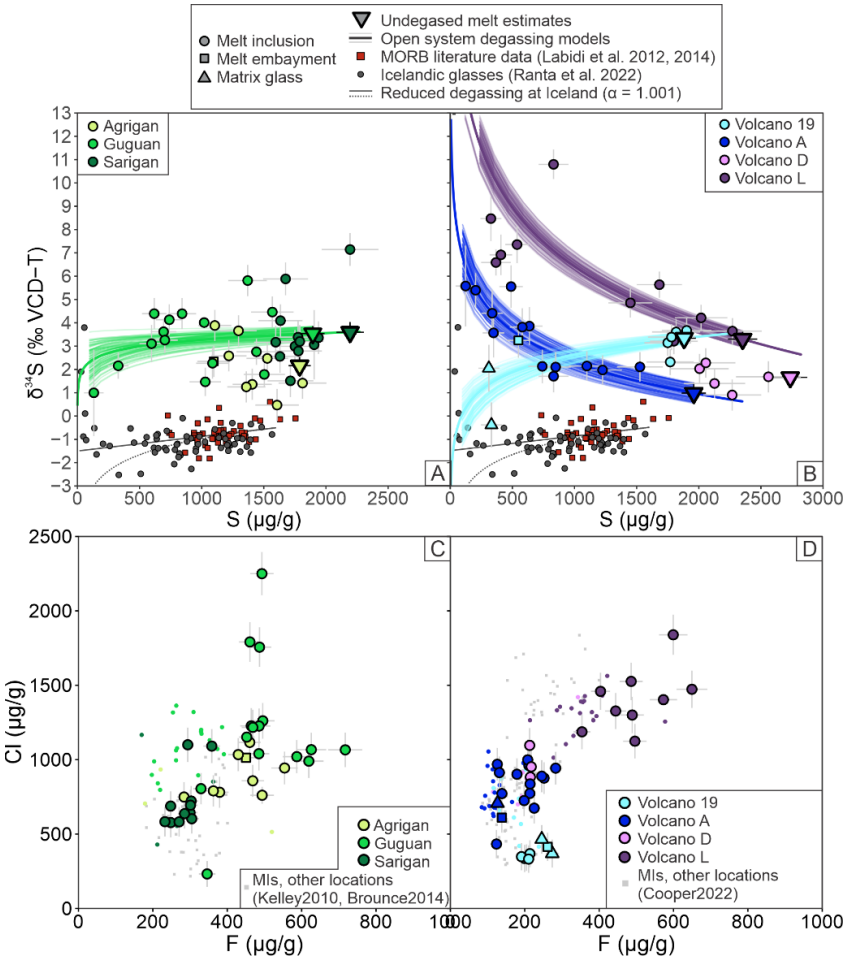

Fig. 2. Sulphur isotope ratios measured in Marianas (A) and Tonga glasses (B) plotted against sulphur content. Open system equilibrium degassing models are also shown (coloured curves), alongside literature data available from reduced MORB and Icelandic glasses. Undegassed melt $\delta^{34}S$ estimates are also shown for each locality (large triangles). Chlorine vs. fluorine concentrations in Mariana (C) and Tonga (D) glasses. Error bars are 1σ. Sources of literature data are indicated in the figure legends.

References

[1] Cooper et al. (2022) Journal of Petrology, **63(8)**, egac072.
[2] Brounce et al. (2014) Journal of Petrology, **55(12)**, 2513-2536
[3] Syracuse et al. (2010) Physics of the Earth and Planetary Interiors **183(1-2)**, 73-90.
[4] Beaudry & Sverjensky (2024) Geochemistry, Geophysics, Geosystems, 25(7), e2024GC011542

Constraining magmatic volatile fluxes and storage dynamics during the post glacial period at an active arc volcano

H. Thornhill[1], D. Ferguson[1], A. Macente[2], F. Boschetty[1], E. Morgado[3] & J. Harvey[1]

[1]School of Earth and Environment, University of Leeds, Leeds LS2 9JT, UK
[2]School of Civil Engineering, University of Leeds, Leeds LS2 9JT, UK
[3]Escuela de Geología, Universidad Mayor, Santiago, Chile

Motivation

Arc magmatism takes place at subduction plate margins, where elemental cycling occurs between the Earth's surface and interior [1]. This magmatism allows the transport of carbon from the deep, solid earth (primarily derived from the subducted slab) to the surface (released via arc volcanism). This 'deep carbon cycle' regulates long-term planetary habitability by maintaining atmospheric CO_2 levels [2]. Constraining the source of arc magmatism and temporal-spatial variations in volcanogenic CO_2 flux from arc volcanoes, is critical to understanding the deep carbon cycle and its role in the Earth System [3]. Accurately determining the carbon content of magma is challenging and requires multi-technique analyses. In this project we aim to constrain volatile contents and storage dynamics for magmas erupted from an active arc volcano (Mocho-Choshuenco, Chile). The activity at this volcano is thought to have been influenced by glacial activity, and there is evidence of variable magmatic sources and elevated CO_2 contents [4,5,6,7,8].

To investigate the dynamics of the magmatic system feeding this volcanic complex, we utilise olivine-hosted melt inclusions. These small pockets of trapped melt (now silicate glass) sample magma from deep within the plumbing system, retaining magmatic volatiles that would otherwise be lost to degassing. Volatile-rich bubbles are common within melt inclusions. These can contain >90% of the total inclusion CO_2, and require separate analytical methods such as Raman Spectroscopy [10, 11, 12].

The results of Secondary Ionisation Mass Spectrometry (SIMS) on inclusion glass, performed at the Edinburgh Ion Microprobe Facility (EIMF), are combined with inclusion and bubble volumes determined from X-ray Computed Tomography (XCT), and bubble CO_2 density derived from Raman Spectroscopy to recreate total melt inclusion CO_2 contents. This combination of analytical techniques results in some of the most precise CO_2 contents for bubble-bearing melt inclusions to date, due to improvements in inclusion volume measurements afforded from XCT analysis [13, 14, 15]. In addition to melt inclusion volatile content, trace element concentrations were also collected to provide an insight into magma source and variation between the eruption units sampled.

Samples and Methodology

Inclusion-bearing olivine crystals were selected from loose scoria collected from the flanks of Mocho-Choshuenco during a field campaign in January 2023. The volcano has produced a large volume of compositionally variable eruptions since the last regional glaciation (c.a. 18ka), with notable differences in explosivity, eruption style, geochemical signatures, and elevated CO_2 contents [4,5,6,7,8]. Samples for this study were collected from 11 of the main post-glacial eruptive units as defined in [4], to investigate the dynamics of the magma system and volatile contents of each eruption. Crystals were polished to expose melt inclusions, then mounted in epoxy grain mounts for analysis. Prior XCT scans and Raman Spectrometry had been undertaken at the University of Leeds.

Melt inclusions were analysed at the EIMF on the Cameca IMS 7f-Geo over the course of a week in November 2024. Volatile concentrations (H_2O and CO_2) were collected in the first analytical runs, followed by a second run where 18 different trace elements were collected from the same inclusions. Volatile measurements in olivine hosts were taken sporadically throughout the analysis to constrain a background level, along with standards analysed prior to each run for calibration. An internal glass standard was also included in each epoxy block, analysed alongside samples as an internal control.

Results and Discussion

In total, 164 melt inclusions were analysed from 11 different eruption deposits. Subsequent data evaluation along with BSE imaging shows that some analysis spots missed the intended inclusion target, along with some extensive post entrapment crystallisation of inclusions. These data points have been removed from the original dataset, leaving only homogeneous glass inclusion data (total: 119). Major element analysis of the inclusion glass is yet to be completed, and therefore absolute totals for trace element contents cannot be corrected for composition or post entrapment crystallisation.

The data collected shows clear variability in the CO_2 content from different eruptions, with maximum contents of around 1400ppm (fig 1a). The two most recent eruptions studied appear to have lower inclusion glass CO_2 contents in comparison to earlier eruptions. In particular, unit MC23 has a very low average of just 66 ppm, perhaps indicating that inclusions were trapped after degassing. There is also a difference in trace element ratios in some eruptions, with the earliest (MC1) having significantly elevated La/Yb ratios, commonly indicative of a lower degree of partial melting (fig 1b). MC15 and MC21 also appear to have been influenced by this signature, with a wide range in trace element compositions, reaching similar La/Yb values to MC1 in some inclusions. This could reflect crystallisation and inclusion entrapment in different magma reservoirs, suggesting at least two variable magma sources. These data will be combined with Raman, XCT and EPMA for further investigation and CO_2 quantification.

References

[1] Hayes, J. and Waldbauer, J. (2006). Phil. Trans. R. Soc. B. 361(1470), 931-950. [2] Wong, K. et al. (2019). Front. Earth Sci. 7, 263. [3] Huybers, P. and Langmuir, C. (2009). Earth and Planetary Science Letters. 286(3-4), 479–491. [4] Rawson, H. et al. (2015). Journal of Volcanology and Geothermal Research. 299, 103–129. [5] Rawson, H. et al. (2016a). Earth and Planetary Science Letters. 456, 66–77. [6] Rawson, H. et al. (2016b). Geology. 44(4), 251–254. [7] Mallea-Lillo, F. et al. (2022). Journal of South American Earth Sciences. 117, 103875. [8] Feignon, J. et al. (2022). Bull Volcanology. 84(4), 40. [10] Wallace, P. et al. (2021). Annu. Rev. Earth Planet. Sci. 49(1), 465-494. [11] Moore, L. (2015). American Mineralogist. 100(4), 806-823. [12] Wieser, P. et al. (2021). Geochem Geophys Geosyst 22(2). [13] Hanyu, T. et al. (2020). Chemical Geology. 557, 119855. [14] Tucker, J. et al. (2019). Geochimica et Cosmochimica Acta. 254, 156-172. [15] Van Gerve, T. et al. (2024). Journal of Petrology. 65, 1-24.

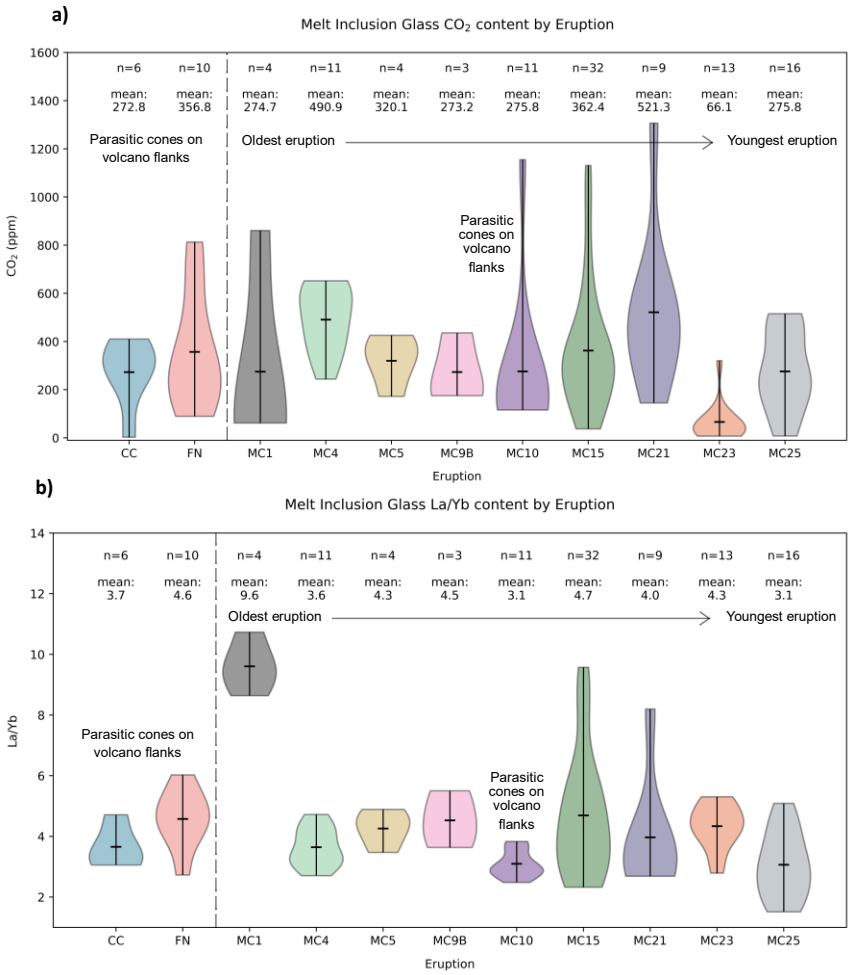

Fig. 1. (a) Melt inclusion CO_2 contents, showing the distribution of measurements within each unit sampled and the average CO_2 content for each eruption. (**b)** Melt inclusion trace element ratio (La/Yb) highlighting a distinct signature in MC1. MC15 and MC21 also appear to have some inclusions with similarly high ratios.